

Tailored Biosensors for Drug Screening, Efficacy Assessment, and Toxicity Evaluation

Yi Tao,* Lin Chen, Meiling Pan, Fei Zhu, and Dong Zhu*

Cite This: *ACS Sens.* 2021, 6, 3146–3162

Read Online

ACCESS |



Metrics & More



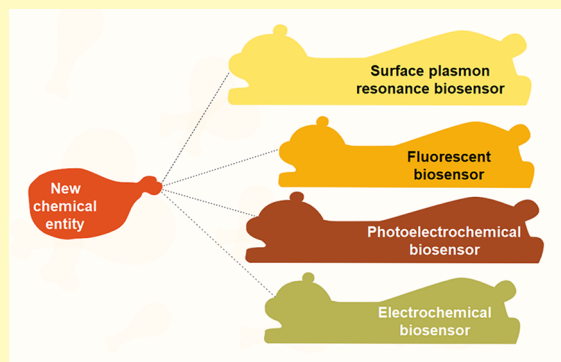
Article Recommendations



Supporting Information

ABSTRACT: Biosensors have been flourishing in the field of drug discovery with pronounced developments in the past few years. They facilitate the screening and discovery of innovative drugs. However, there is still a lack of critical reviews that compare the merits and shortcomings of these biosensors from a pharmaceutical point of view. This contribution presents a critical and up-to-date overview on the recent progress of tailored biosensors, including surface plasmon resonance, fluorescent, photoelectrochemical, and electrochemical systems with emphasis on their mechanisms and applications in drug screening, efficacy assessment, and toxicity evaluation. Multiple functional nanomaterials have also been incorporated into the biosensors. Representative examples of each type of biosensors are discussed in terms of design strategy, response mechanism, and potential applications. In the end, we also compare the results and summarize the major insights gained from the works, demonstrating the challenges and prospects of biosensors-assisted drug discovery.

KEYWORDS: surface plasmon resonance biosensor, bilayer interferometry biosensor, grating coupled interferometry biosensor, switchsense biosensor, fluorescent biosensor, electrochemical biosensor, photoelectrochemical biosensor, drug screening, efficacy assessment, toxicity evaluation



the challenges and prospects of biosensors-assisted drug

The discovery of small-molecule drug can be regarded as a challenging multidimensional problem, in which efficacy and safety of potential candidates need to be optimized.¹ Different enzymatic tests and biophysical assays have been adapted for the needs of drug discovery.² Despite great initial success, bringing new drugs to the market is still a time-consuming and costly process. Besides, existing computational high-throughput methods suffer from a serious problem as their experimental counterparts showed a high false-positive rate.³ In this context, accurate and sensitive biosensors have been considered as a potential solution.⁴

A biosensor is a device with a specific biorecognition element that can interact with an agent in the sample and cause changes in physicochemical properties, which can be converted into a measurable signal.⁵ Nowadays, a plethora of tailored biosensors have become an indispensable part of drug discovery platforms. These tailored biosensors are designed specifically for drug discovery and are constrained by a specific drug target, which have accelerated the evaluation of efficacy and toxicity of potential candidates and enabled drug screening against challenging targets, such as protein–protein interaction.⁶ However, transduction mechanisms, detection mode, strengths, and limitations of these biosensors are different. Supporting Information Table S1 summarizes the characteristics of the biosensors in drug discovery.

Although several excellent reviews^{7–9} have covered label-free optical biosensors ten years ago, the current application of state-of-the-art biosensors in the field of drug discovery has not been summarized yet. Therefore, this review is to introduce the recent progress of biosensors, including surface plasmon resonance, fluorescent, electrochemical, and photoelectrochemical systems. The transducing options of these biosensors function together with suitable nanomaterials, including quantum dots, luminescent carbon dots, graphene oxide, carbon nanotubes, magnetic nanoparticles, nanocrystals, and up-converting nanoparticles fused together and provided extreme variability of existing biosensor options. Applications of these biosensors in drug discovery are critically discussed.

DESIGN OF BIOSENSORS FOR DRUG SCREENING IN VITRO

Screening and locating an appropriate lead structure is the first step in the pipeline of drug discovery. A full characterization of

Received: July 28, 2021

Published: September 13, 2021



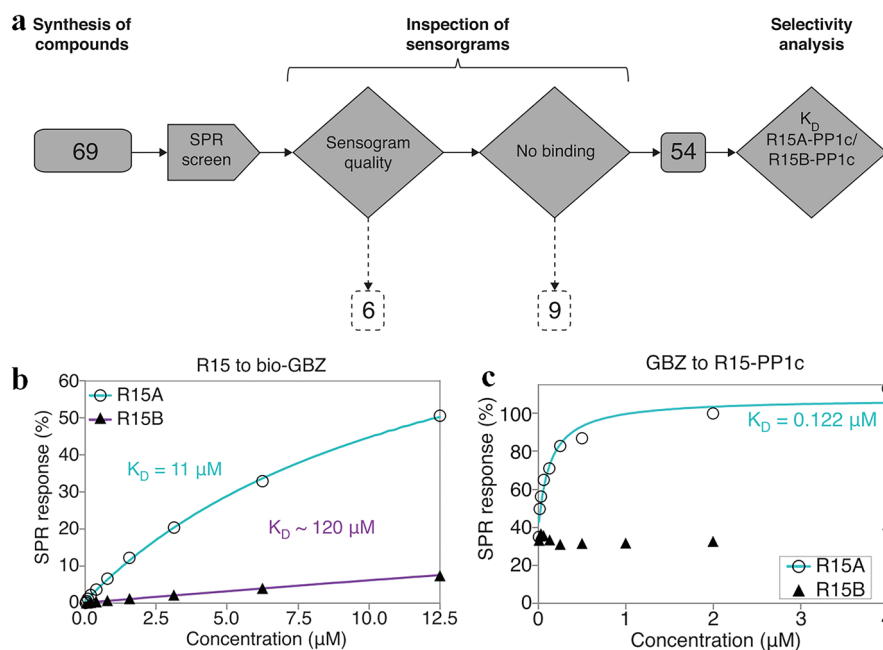


Figure 1. SPR-based assay with reconstituted R15 holophosphatases that measures affinities of R15A inhibitors. (a) Overview of the screening strategy. During the data analysis, compounds were rejected on the basis of sensorgram quality or no binding to either holophosphatase. (b) Normalized steady-state binding curves from SPR showing binding of R15A (cyan) and R15B (magenta) to bio-GBZ immobilized on the streptavidin sensor chip surface. Bio-GBZ (biotinylated GBZ) is an R15A inhibitor as potent as GBZ. (c) Normalized SPR steady-state binding curves showing binding of GBZ to R15A-PP1c (cyan) and R15B-PP1c (magenta) reconstituted on the streptavidin sensor chip surface. Reprinted with permission from ref 17. Copyright 2018 The Authors under Creative Commons International 4.0 license, published by Elsevier.

a lead compound requires two types of HTS-compatible assays: one is functional assays to determine the effect of compounds in terms of signaling, and the other is mechanistic assays to detect the direct effects of compounds on their targets. The interactions between potential candidate and drug target are quantified in terms of binding parameters such as dissociation constant (K_d). To achieve this goal, a variety of biosensors have been developed.

Surface Plasmon Resonance Biosensors. Surface plasmon resonance (SPR) biosensors become a golden standard for studying drug–target interactions and provide a huge stage for drug screening. There are two major challenges for SPR. One is the way of immobilization. It must keep the ligand-binding ability of the protein after covalent attachment to the biosensor surface. The other is the expertise that is required to set up a high-quality SPR bioassay. The number of drug screenings with SPR biosensor is steadily increasing, and these examples have been summarized in Table S2, covering a wide range of drug targets, i.e., metallo- β -lactamase VIM-2,¹⁰ clostridial collagenases,¹¹ tumor necrosis factor receptor, signal transducer and activator of transcription 3,¹³ C-X-C chemokine receptor type 4,¹⁴ α -glucosidase,¹⁵ FK506-binding protein,¹⁶ R15B-PP1c holoenzyme,¹⁷ PI3K γ ,¹⁸ xanthine oxidase,¹⁹ DNA MTase,²⁰ and so on. SPR technology has been extended to difficult target types, such as membrane-bound proteins. For the purpose of preserving the conformation and activity of the surface-bound proteins, novel reconstitution and tethering methods are necessary.

Advantages of Surface Plasmon Resonance Biosensors. The equilibrium constants of interactions between drug targets and potential candidates play a pivotal role in establishing the duration of clinical benefit of potential candidates. SPR biosensor offers information not only on the binding kinetics between drug targets and potential candidates

but also on the affinity as well as the drug interaction through the use of reference compounds/substrates/binding partners or binding site-directed mutations in the binding site. For instance, one project¹¹ selects collagenase H (ColH) domain as the drug target and establishes an SPR-based screening method against 1520 kinds of molecules. In order to validate the integrity of the immobilized ColH structural domain, FALGPA, a collagenase-specific peptidic substrate, has been utilized. Meanwhile, compounds with a higher normalized response than the substrate at 500 μ M are considered as hit compounds. In another project,²¹ it combines SPR biosensor and site-directed mutagenesis of LANCL2 proteins (single mutant R118I and triple mutants R118I/S41A/E46I and R118I/R22I/K362I) for site-specific binder screening. Finally, it obtains a high-affinity abscisic acid-binding site R118, with a K_D of 2.6 nM. In addition, the SPR biosensor is compatible with drug screening mixed with complex herbs. As is known to all, herbs contain tens of thousands of inactive components, which may interfere with the detection of SPR. However, a group utilized the SPR biosensor to screen for inhibitors against multiple transcription factors in herbal mixtures, including STAT3, CXCR4, and TNF.^{12–14} These works validate that inactive component in herbal mixtures cannot affect response signals in SPR, which do not interfere with the detection of bioactive components.

Disadvantages of Surface Plasmon Resonance Biosensors. The application of the SPR biosensors for drug screening necessitates a far more suitable immobilization strategy. One group¹⁰ adopts SPR biosensors as the primary screening method and takes a biochemical assay as the secondary screening method to select Verona integron-encoded metallo- β -lactamase (VIM-2) inhibitors against a library of 490 fragments. It is worth noting that such a screening strategy is able to avoid false-positive hits caused by

pan assay interference compounds. Nevertheless, it is estimated that 65% of the covalently immobilized VIM-2 is inactive, revealing that positive controls must be utilized first to ensure the ligand-binding competence of the protein on the surface of the SPR biosensor. Isolated protein domains are adequate for the ligand-binding experiment albeit with the loss of full functionality. Another group¹⁷ reports an SPR-based screening strategy for the identification of selective inhibitors of allophosphatases from the synthesized compounds (Figure 1a). Compounds are ruled out due to the quality of the sensorgram or the lack of binding to any of the allophosphatases. Notably, there exists a huge difference between the measured 11 μM affinity of R15A for biotinylated GBZ (Figure 1b) and the sub-micromolar potency of GBZ in cells. However, when both catalytic subunit PP1c and regulatory subunit R15 are reconstituted on the SPR chip, the measuring result of affinity of GBZ for R15A is 0.122 μM , consistent with the results of the cellular assay (Figure 1c). The limitation of some isolated regulatory subunits lies in the fact that these regulatory subunits are intrinsically disordered. Therefore, it is of great importance to select the correct coupling method for SPR.

Standard immobilization techniques such as amine-coupling, Ni-NTA capture, and streptavidin–biotin capture are available for SPR.⁷ Amine-coupling is considered as an extremely convenient method for immobilizing proteins, which requires activation of the chip surface by adding a mixture of *N*-hydroxysuccinimide (NHS) and 1-ethyl-3-(3-(dimethylamino)propyl)carbodiimide (EDC). The amine-coupling method requires that the protein be dissolved in a low-salt buffering liquid which is at least one pH unit lower than the protein's pI. Binding parameters of amine-coupled proteins match well with those of proteins in completely free states. However, the protein is susceptible to denaturing conditions and the coupling buffers. The next most straightforward coupling method is the streptavidin–biotin capture method. In this method, a biotinylating agent such as sulfo-succinimidyl 6'-(biotinamido)-6-(hydroxylamino)-hexanoate reacts with primary amine groups in proteins. Then, the biotinylated protein is desalted and recovered before being captured on avidin prederivatized chips. The spacer arm of the biotinylating agent gives the protein more opportunities to rotate as if it were free in solution. Additionally, there is also a wide range of other immobilization methods, such as antitarget antibody–target-coupling method and metal ion–polyhistidine sequences coordination coupling method. Antitarget antibody–target-coupling may complicate ligand identification as the ligand may also bind to the antibodies. Besides, some researchers have added several polyhistidine sequences into the N- or C-terminus of protein which can be coupled to Ni²⁺-NTA chips. The merit of this coordinated metal ion–polyhistidine sequences coordination coupling approach is that the protein can be readily removed from the surface by using EDTA stripping. What's more, the chip can be recharged by injection of nickel ions, and new fresh protein can be captured.

Optical Waveguide Grafting Biosensors. Optical waveguide grating (OWG) biosensors takes advantage of resonant waveguide gratings or nanostructured optical gratings to identify binders of target proteins.²² Planar waveguide systems and microplates increase the yield of drug screening and ensure the data quality. The OWG biosensors have been applied to drug targets (Table S3), including muscarinic M3 receptor,²³ muscarinic acetylcholine M2 receptor,²⁴ G-protein-activated

inwardly rectifying potassium channels²⁵ and cannabinoid receptors.²⁶

Advantages of Optical Waveguide Grafting Biosensors. In contrast to sequentially operating systems, OWG biosensor provides much more throughput and is capable of detecting weak interactions between small molecules and drug targets. OWG biosensor can also enable one to monitor real-time cellular responses when subjected to the influence of compounds.

Disadvantages of Optical Waveguide Grafting Biosensors. The modified sensor surface of OWG biosensor is only used in one binding experiment. Compared with the SPR-based method, the OWG biosensor consumes larger amounts of target protein. Moreover, this plate-based platform is usually operated in equilibrium, which only performs for K_d determination.

Biolayer Interferometry Biosensors. Biolayer interferometry (BLI) biosensor is microfluidic-free. It analyzes the interference pattern of white light reflected from a layer of immobilized drug targets on the tip of a biosensor against an internal reference.²⁷ It can get real-time data of affinity, kinetic parameters, and concentration. Table S4 shows several major cases of the application of BLI biosensors for drug screening. The drug targets cover glutamate carboxypeptidase II,²⁸ glutaminase,²⁹ double-stranded DNA,³⁰ and protein–protein interactions, such as tissue transglutaminase and fibronectin interaction,³¹ and SARS-CoV-2 RBD and hACE2 interaction.³²

Advantages of Biolayer Interferometry Biosensors. Biolayer interferometry biosensor is only minimally affected by changes in the medium, since it does not measure refractive index or dielectric constant of the solution. Meanwhile, a range of biosensor tips can be dipped into an analyte solution, and then the analyte is evaluated in parallel.

Disadvantages of Biolayer Interferometry Biosensors. Compared with SPR-based methods, BLI biosensors have less sensitivity and higher reagent consumption.

Grating Coupled Interferometry Biosensors. Similar to SPR, grating coupled interferometry (GCI) biosensor detects refractive index changes near the sensor surface, which is ascribed to massive changes induced by the formation of ligand–target complexes.²⁷ This discovery assists in measuring kinetic rates and determining affinity constants of interacting ligands quickly and accurately. Table S5 summarizes the latest applications of GCI biosensors in drug screening. The drug targets include bovine serum albumin³³ and carbonic anhydrase II.³⁴

Advantages of Grating Coupled Interferometry Biosensors. The sensitivity of GCI biosensor is superior to the greatest performance of surface plasmon resonance.³³ The capabilities of the GCI biosensor ranged from weak binding molecule drugs to binding analysis at slow dissociation kinetics.

Disadvantages of Grating Coupled Interferometry Biosensors. The GCI biosensor requires expertise to choose suitable chips for interaction experiment as some ligands may bind nonspecifically to the chip surface.

Switchsense Biosensors. Switchsense biosensor is based on short DNA nanolevers in a microfluidic channel.³⁵ On the gold surface, the negatively charged DNA nanolevers can be electrically actuated (“switched”) to oscillate at high frequencies. In order to conduct the screening, the compounds have to be cross-linked to the DNA strand. The binding of compounds to drug targets affects the hydrodynamic friction of the DNA nanolever, which can be detected by using time-

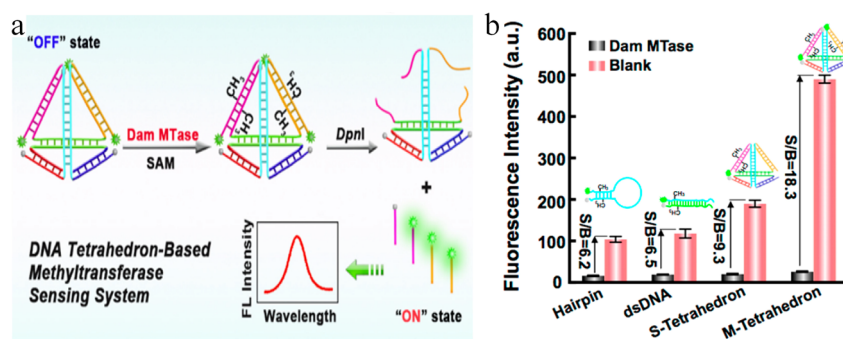


Figure 2. DNA tetrahedron based FRET biosensors for screening DNA MTase inhibitors. (a) Schematic representation of “off–on” fluorescence sensing system with DNA tetrahedron. (b) Fluorescence signals of different probes (500 nM) in the mixture of buffer before and after addition of DNA MTase. S/B indicates the signal-to background ratio. Reprinted with permission from ref 47. Copyright 2017 American Chemical Society.

resolved single-photon counting.³⁶ Only 40 μL of 250 nM ligand–DNA conjugate will be consumed for one experiment. As a new technology, application of switchsense biosensor for drug screening is still extremely rare. One successful case is NAD^+ -dependent lysine deacetylase Sirt2.³⁷

Advantages of Switchsense Biosensors. Switchsense biosensor is suitable for high content analysis. Binding kinetics and conformational changes of proteins, small molecules–drug target interactions, and enzymatic activity can all be realized by using the switchsense biosensor. Meanwhile, the biosensor requires only a small quantity of sample volume (50 μL).

Disadvantages of Switchsense Biosensors. It is possible that nonspecific binding to double-stranded DNA on the surface will occur, especially for drug targets. Application of the technology to drug discovery required expertise to carry out the experiment and to interpret complex interactions. In addition, the biosensor is not suitable for high-throughput screening because the regeneration rate of chip is relatively slow.

Förster Resonance Energy Transfer Biosensors. Fluorescence assay is widely applied for its high sensitivity and economical benefits in the HTS test. However, the testing results of fluorescence intensity are always influenced by the environment. Meanwhile, fluorescence polarization requires a tool to adjust the size of the fluorophore-containing moiety. This tool usually has a narrow testing signal channel. Unlike the former fluorescence-based biochemical assay, FRET-based biosensors are only determined by the distance between donor and acceptor fluorophores.³⁸

Typical FRET fluorophore is covered with ultraviolet dyes and near-infrared (NIR) dyes. The former one included coumarin-, naphthalene-, and pyrene-based analogues, while the latter consists of cyanine (e.g., Cy3, Cy5, Cy5.5, Cy7, and Cy7.5), and rhodamine.³⁹ As for FRET biosensors, an ideal target may be the drug target that can cut the linkage between the donor or acceptor fluorophores. The applications of FRET biosensors for drug discovery have increased annually (see Table S6). A multitude of drug targets have been targeted, including acetylcholinesterase,⁴⁰ tyrosinase,^{41,42} HIV-1 reverse transcriptase,⁴³ α -glucosidase,⁴⁴ cereblon,⁴⁵ DNA MTase,^{46–48} RNase H,⁴⁹ RNase A,⁵⁰ β -secretase,⁵¹ protein kinase A (PKA),⁵² amyloid- β ,⁵³ CBP BrD,⁵⁴ and hNTH1-YB1 complex.⁵⁵ Moreover, protein–protein interactions have also been targeted, such as SERCA2a-PLB interaction.⁵⁶

Advantages of Förster Resonance Energy Transfer Biosensors. FRET is a process of nonradioactive energy transfer between the donor–acceptor pairs. Compared with

radioactive assays, FRET is a reliable method, and waste handling cannot be a tricky issue anymore. At the same time, FRET-based small-molecule probes can be quickly absorbed by cells and have the potential for in situ detection. Therefore, the application of FRET biosensors provides the investigator with plenty of scope.

Disadvantages of Förster Resonance Energy Transfer Biosensors. Most of the typical small-molecule fluorophores, such as rhodamine, derivatives of fluorescein, proprietary dyes, and fluorescent proteins, have low Stokes shifts and wide spectra which lead to high background values. For instance, fluorescence spectra and quantum yields of cyanine dyes are affected by nonspecific protein binding, excess aggregation, and photobleaching.⁵⁷ The properties of high hydrophobicity and Stokes shifts of BODIPY dyes greatly limit their applications in FRET assay.⁵⁸ In addition, several FRET biosensors have been fabricated by employing the strategy of conjugating organic dyes to enzymes or receptors. The preparation procedure is tedious and time-consuming. One example is the reverse transcriptase (RT) of human immunodeficiency virus-1 (HIV-1).⁵⁹ The production of this FRET biosensor needs to produce a RT mutant with a single accessible cysteine, labels it with Alexa 488, and purifies it in an enzymatically active state.

Integration of Nanomaterials into Förster Resonance Energy Transfer Biosensors. Due to the drawbacks mentioned above, a growing amount of attention has been drawn to the application of quantum dots (QDs), carbon dots (CDs), polymer dots, up-conversion nanomaterials, and AIE dots as FRET acceptor. FRET biosensor is also known as quenching resonance energy transfer (QRET). It takes these nanomaterials as a kind of quenching molecule instead of an acceptor fluorophore, which can achieve more S/B values than that of standard FRET assays.

Compared with conventional organic dyes and fluorescent proteins, semiconductor QDs features outstanding optical properties, such as good photostability, broad excitation, high rate of quantum yield, and narrow emission. The QDs are able to serve as efficient FRET donors instead of conventional organic dyes. The altered spectrum and fluorescence lifetime can serve as an “on/off” switch for detecting the biomolecules. Taking DNA MTase as an instance, aberrant DNA MTase active component is closely associated with a great variety of human malignancies. A single QD-based biosensor is designed for the turn-on detection of DNA MTase⁴⁶ and its inhibitors in order to apply for a hairpin DNA probe, which contained a fluorescence quencher (i.e., BHQ2) at the 5' end and a fluorophore (Cy5) at the opposite strand of the stem. 605QD

is selected as the FRET donor. In comparison to the QD-free assay, a 5-fold increase in S/B ratio is observed for the single QD-based biosensor (34.17 versus 7.59). Another group researches different DNA substrates reacting to DNA MTase sensors.⁴⁷ In this process, it can be found that the S/B ratio of DNA tetrahedron nanostructures increases three times more than that of DNA hairpin (see Figure 2a,b). Additionally, Y-shaped DNA substrate tandem concatenated hybridization chain reaction is also utilized for DNA MTase sensing. However, both biosensing mechanisms have two enzymes, i.e., DNA MTase and DpnI. It is worth noting that the compounds working on DpnI may also be counted as the DNA MTase inhibitors. The specificity of the biosensor needs to be studied in-depth.

Except for semiconductor QDs, CDs also show outstanding performances, such as excellent photostability, favorable biocompatibility, environmental friendliness, and favorable price. A FRET biosensor utilized a nitrogen-doped CDs and cobalt oxyhydroxide nanoflakes as the quencher.⁴⁴ The fluorescence intensity of CDs decreases significantly when the concentration of CoOOH is increased from 0 to 0.6 mM. The FRET biosensor was described for screening of α -glucosidase inhibitors from natural product. Two kinds of α -glucosidase inhibitors are identified, i.e., maslinic acid and oleanolic acid. However, IC₅₀ values of the two compounds are above 10 mM, which are much too high for hit compounds. Its positive control acarbose is 55.7 μ M. In our opinion, the IC₅₀ value of hit compounds should be observed at micromolar or even lower concentrations.

Besides nanoflakes, other nanomaterials, such as gold nanoclusters (AuNCs), polymer nanoparticles, and graphene oxide, have been gathered into FRET for drug screening. AuNCs@11-mercaptopundecanoic acid-Cu²⁺ ensemble-based fluorescent biosensor is designed for screening inhibitors against acetylcholinesterase (AChE).⁴⁰ The titration of Cu²⁺ into the solution of AuNCs resulted in a gradual fluorescence quenching as the concentration of Cu²⁺ is increased from 0 to 5000 nM. Meanwhile, it adds AChE and ATCh. After that, TCh comes out. Subsequently, TCh captures Cu²⁺ ions and turns on fluorescence of AuNCs@11-MUA. It is obvious that the specificity of the AuNCs@11-MUA-Cu²⁺ ensemble-based sensing mechanism works well. On the basis of this FRET biosensor, the IC₅₀ value of the positive control tacrine is determined to be 2.8 nM.

Transformation into Time-Resolved Förster Resonance Energy Transfer Biosensors. In order to achieve superior sensitivity and assay robustness, shifting the form of FRET assay into a TR-FRET format is a practical way. For G-protein-coupled receptors (GPCRs) and receptor tyrosine kinases (RTKs), FRET biosensors are hampered by the low signal-to-noise ratio due to the small conformational changes of receptors that occur upon activation. To work it out, TR-FRET mechanism, possessing rare earth lanthanides cations such as terbium and europium, has become the cutting-edge technique for sensing receptors.⁶⁰

Advantages of Time-Resolved Förster Resonance Energy Transfer Biosensors. TR-FRET shows distinct advantages over other HTS screening technologies and over other fluorescent techniques. First, a delay of 50–150 μ s between the excitation and measurement of the emission signal ensures that background fluorescence is greatly decayed. Second, lanthanide's narrow peaks in fluorescence emission spectra lay a strong foundation for S/B. Third, its combination

of high sensitivity and robustness achieves miniaturization, even up to a 1536-well plate format. A reduced quantity of lanthanide-labeled entities saves a lot of energy in an HTS procedure. Taking the homodimeric mGlu2 receptor as an example,⁶⁰ a SNAP-tag is conjugated to the N-terminus of each subunit of the receptor in order to detect conformational changes upon agonist or antagonist activation. A typical FRET pair (Atto 488 and red) leads minor changes in FRET activation, while TR-FRET-compatible fluorophores (terbium) bring in huge changes in signal upon receptor activation. The greatest change in TR-FRET efficiency of SNAP-mGlu2 is made by using SNAP-green as acceptor. Moreover, the ratio of sensitized acceptor emissions integrated in time channel 2 (50–100 μ s) and channel 3 (1200–1600 μ s) leads to the biggest variations. This TR-FRET biosensor enables one to measure easily the potency of hit compounds over homodimeric mGlu2 receptor and could be extended to a wide range of cell surface receptors, including γ -aminobutyric acid receptor (GABA_B), luteinizing hormone receptor (LH), class B parathyroid hormone receptor-1 (PTH), epidermal growth factor receptor (EGF), and insulin receptors (IRs). Most significantly, the potencies of a series of agonists obtained by using this TR-FRET biosensor have a close relation with the data of functional assay. This work not only provides a versatile strategy for developing conformational biosensors of receptors for high-throughput screening but also illuminates the versatility of the TR-FRET biosensors.

Disadvantages of Time-Resolved Förster Resonance Energy Transfer Biosensors. Unfortunately, a few drawbacks still exist in TR-FRET biosensor. It is still less sensitive than radioactive assays, and it can be cumbersome to develop TR-FRET-compatible fluorescent ligands that retain a good affinity for the target. In the same way, the labeling of the target with TR-FRET fluorophores is not always easy to be achieved. In the case of GPCRs, it is often necessary to modify the receptor, which could affect its properties. There is still a tricky challenge because of the occurrence of technology hitters and the change in probe properties due to incorporation of labels. Finally, the range of linearity for some quantitative assays is limited, and assays are often more expensive than those based on genetically encoded fluorescent proteins or classical fluorophores.

Aggregation-Induced Emission Based Biosensors. Common fluorophores have the aggregation-caused quenching (ACQ) effect. In contrast, aggregation-induced emission (AIE) biosensors are non-emissive when molecularly dissolved in solution but are induced to emit efficiently by aggregation.⁶¹ A plethora of AIE biosensors have been fabricated for sensitive detection of metal ions, sugars, proteins, or anions.⁶² They depended on weakly fluorescent AIE fluorogens in solutions to interact with protein substrates or oppositely charged chemical to the formation of fluorescent complexes. Upon enzyme digestion, the complexes released the AIE fluorogens back to the solutions, which resulted in aggregation and fluorescence turn-on. The fluorescence turn-on of AIE biosensors was ascribed to the restriction of the intramolecular rotations (RIRs) and restriction of intramolecular vibration (RIV).⁶² AIE materials cover TPE, cyano-substituted stilbene,⁶³ hexaphenylsilole (HPS),⁶⁴ triphenylamine (TPA) derivatives,⁶⁵ 10,10',11,11'-tetrahydro-5,5'-bidibenzo[*a,d*][7]annulenyldiene (THBA),⁶⁶ and tetraphenylsilole.⁶⁷ Remarkably, these AIE biosensors have been used for screening inhibitors against various drug targets (Table S7), such as caspase-3,^{68,69} caspase-

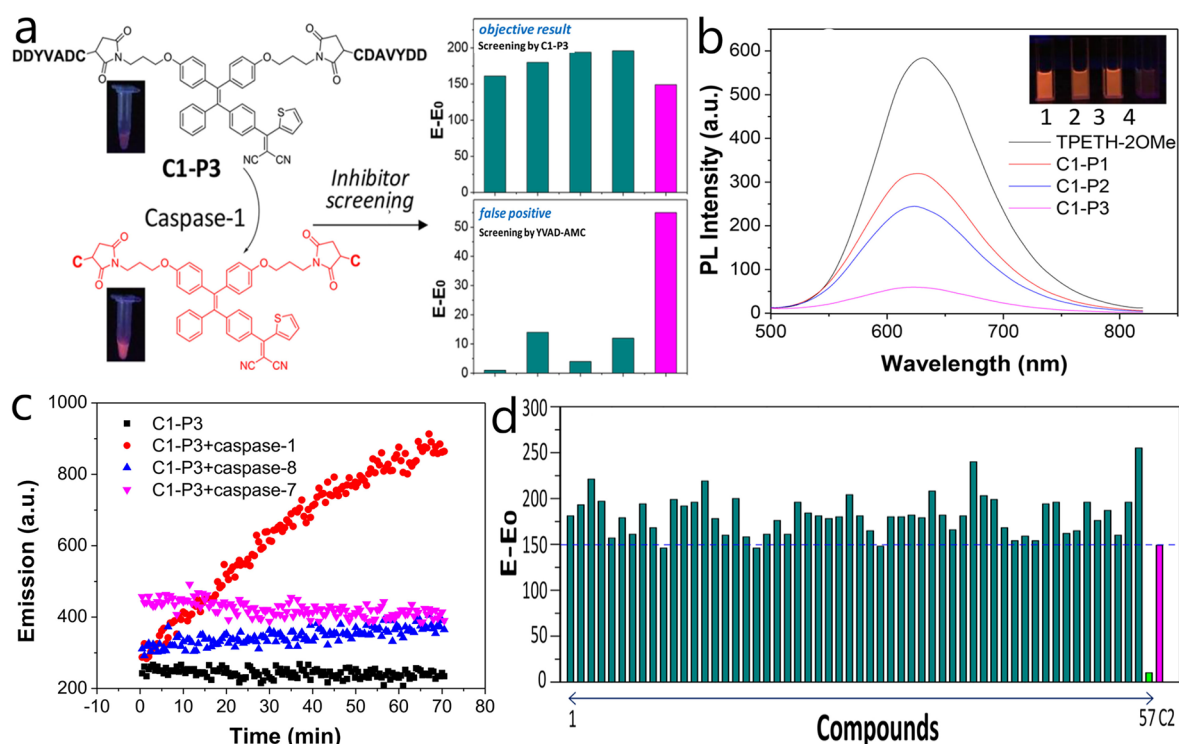


Figure 3. Aggregation-induced emission biosensors for screening caspase-1 inhibitors. (a) Schematic illustration of the aggregation-induced emission biosensors. (b) Emission spectra of three probes in DMSO/HEPES buffer (ex, 420 nm). The insets are the fluorescent photographs of probes in DMSO/HEPES buffer (1:99): (1) for TPETH-2OMe, (2) for C1-P2, (3) for C1-P1, and (4) for C1-P3. (c) Fluorescence intensity of C1-P3 upon incubation with caspase-1, caspase-7, and caspase-8, which was then measured by microplate reader (ex, 420 nm; em, 630 nm). (d) Screening results by C1-P3. Compounds from 1 to 56 are coumarin-originated natural products. Compound 57 (green color) is AcYVAD-CMK, a reference inhibitor to caspase-1. C1 and C2 are the controls (pink color) with probes and caspase-1 only. E_0 is the first acquisition of fluorescence intensity after the addition of C1-P3. E is the fluorescence intensity of the mixture at 10 min after addition of C1-P3. The value of $E - E_0$ below the blue dashed line indicates the corresponding compound possessed potential inhibition toward caspase-1. Reprinted with permission from ref 76. Copyright 2018 American Chemical Society.

7,⁶⁸ histone deacetylase (HDAC),⁷⁰ angiotensin converting enzyme (ACE),⁷¹ telomerase,⁷² SIRT1,⁷³ monoamine oxidase-A,⁷⁴ dipeptidyl peptidase-4 (DPP-4),⁷⁵ caspase-1,⁷⁶ and sialidases.⁷⁷

Advantages of Aggregation-Induced Emission Biosensors. AIE biosensor was superior to the conventional 7-amino-4-methylcoumarin (AMC)-based fluorescent biosensor, because it could rule out false positives derived from coumarins. Natural products exhibited various biological effects.⁷⁸ However, coumarin-originated natural products shared a similar excitation and emission with AMC of conventional fluorescent biosensor (Ac-YVAD-AMC), which could generate false-positive results. To overcome this hurdle, a new tetraphenylethylene–thiophene (TPETH)-based AIE biosensor was fabricated (Figure 3a). Three kinds of hydrophilic peptides were attempted to conjugate to the TPETH on the basis of a thiol–ene reaction.⁷⁶ C1-P3 with two sequences of DDYVAD was selected because it was almost nonfluorescent in the buffer (Figure 3b). Meanwhile, the specificity of C1-P3 was good. Although C1-P3 exhibited high affinity for caspase-8 and caspase-7, it could not be degraded by these enzymes (Figure 3c). The established AIE biosensor was employed for screening caspase-1 inhibitors from coumarin-originated natural products. The conventional screening assay based on Ac-YVAD-AMC revealed that 30 compounds may be potential candidates for caspase-1. However, only three compounds were identified by using the new biosensor (Figure 3d). Twenty-seven of the “hits”

belonged to false positives, which could not inhibit caspase-1’s function. This work highlights the superior advantage of AIE biosensor for drug screening from natural products.

Disadvantages of Aggregation-Induced Emission Biosensors. Plenty of specific peptide sequences linking to a AIE fluorogens as a recognition unit had been synthesized. However, not all of the peptide linked AIE fluorogen functioned well. For instance, TPE-KFPG, TPE-KFPE, and TPE-GPD were synthesized and attempted as biosensors for DPP-4 inhibitor screening.⁷⁵ Interestingly, only TPE-KFPE probe demonstrated significant fluorescence turn-on effect in the presence of DPP-4. Thus, construction of peptide substrate should be considered carefully in order to achieve significant AIE effect. Meanwhile, peptides conjugated AIE biosensors were prone to degradation, which may require special storage conditions. In addition, the AIE biosensors mainly utilized short-wavelength emission at 450–630 nm, which limited its further applications in vivo that demand deep penetration.

Other Fluorescent Biosensors. Several groups have developed other fluorescent biosensors for drug discovery against multiple drug targets (see Table S8), including estrogen receptor (ER),⁷⁹ γ -glutamyl transpeptidase (GGT),⁸⁰ β -glucuronidase,⁸¹ matrix metalloproteinases (MMPs),⁸² histone acetyltransferases (HATs),⁸³ aldehyde dehydrogenases (ALDH),⁸⁴ Hsp 90,⁸⁵ fibroblast activation protein (FAP α),⁸⁶ tyrosinase (TYR),^{87,88} glutaminase (GLS1),⁸⁹ ectonucleotide pyrophosphatase/phosphodiesterase 1 (ENPP1),⁹⁰ sirtuin defatty-acylase,⁹¹ histone deacetylases

(HDACs),⁹² protein tyrosine phosphatase 1B (PTP1B),⁹² and penicillin G acylase (PGA).⁹³

Electrochemical Biosensors. Electrochemical biosensors are portable, self-contained, and low cost. The convergence of functional nanomaterials and microfabrication of electrodes serves as an efficient strategy for creation of electrochemical biosensors for screening inhibitors against multiple drug targets with the detection limits of nano- or femtomolar or even lower concentrations, including DNA MTase,^{94–96} PKA,^{97–99} α -glucosidase,¹⁰⁰ poly(ADP-ribose) polymerase,¹⁰¹ thrombin,¹⁰² and histone acetyltransferases (HATs)¹⁰³ (see Table S9).

Advantages of Electrochemical Biosensors. The required hardware of electrochemical biosensors is cost-effective, uncomplicated, and easy to miniaturize. Electrode materials including noble metals, carbon, and conductive polymers provide various choices for fabrication of the electrochemical biosensors that enable specific applications.⁵

Glassy carbon, as a routine carbon material, shows wide application in electrodes. In order to enlarge the superficial area and conductivity, the surface of the cleaned glassy carbon electrode was functionalized with AuNPs/ERGO hybrids membrane.⁹⁵ Meanwhile, the hybridization of DNA1 and DNA2 triggered the HCR process, leading to the formation of dsDNA superstructures. Then, the cytosine-rich sequences served as an effective template for AgNCs synthesis, which amplified the electrochemical signal. Two model inhibitors, gentamycin and 5-fluorouracil were found to inhibit 50% DNA MTase at a concentration between 1 and 100 μ M. This work revealed multiple amplification strategies could guarantee the high sensitivity of electrochemical detection.

Disadvantages of Electrochemical Biosensors. Electrode fouling is one of the main disadvantages, leading to a loss of sensitivity and selectivity of the electrochemical biosensor. Meanwhile, molecules of the sample matrix that undergo electrochemical reactions with the electrode will lead to false-positive signals. As a typical example, carbon electrode works best with organic redox molecules, but their inherent reactivity may be prone to nonspecific reactions in complex sample matrixes.^{104,105} Moreover, ITO electrode remains unstable in acidic environments. Besides, none of the above electrochemical biosensors were compatible with high-throughput screening.

To overcome this hurdle, a new high-throughput electrochemical assay was created by the oxidative trapping of the transketolases–thiamine pyrophosphate intermediate.¹⁰⁶ Of note, 96 electrochemical assays were accomplished in parallel in only 7 min. It was applied to screen against an in-house chemical library of 1360 molecules. One potential hit compound was picked out with an IC_{50} value of 63 μ M. In contrast to other enzymatic methods, this work not only required one donor substrate and a low amount of enzyme but also was nonsensitive to optical interferences.

Photoelectrochemical Biosensors. Photoelectrochemical biosensors (PECs) own the merits of electrochemical and optical assay.¹⁰⁷ A PEC biosensor consists of an excitation source, a cell, and an electrochemical workstation with a three-electrode system. The applications of PEC in drug discovery cover drug targets (see Table S10) that include DNA methyltransferase,^{108,109} protein kinase,¹¹⁰ thrombin,¹¹¹ and T4 polynucleotide kinase.¹¹²

Advantages of Photoelectrochemical Biosensors. PEC biosensor inherits the advantages of electrochemical biosensor but possesses higher sensitivity due to its unique

PEC setup consisting of total separated energy forms of light and electricity as excitation source and detection signal, respectively. Semiconductor materials such as indium tin oxide (ITO) are cheap, transparent, and easy to process. Compared with gold, they show a larger potential window. One group designed a signal-on photoelectrochemical biosensor for sensing DNA MTase.¹⁰⁸ The ITO electrode surface was coated with anti-5-methylcytosine antibody to capture double-stranded DNA which was methylated by the DNA MTase. Its photocurrent increased gradually as the concentration of M.SssI MTase ramped from 1 to 50 units/mL. Moreover, the IC_{50} value of a positive inhibitor RG108 was determined to be 152.54 nM. In the same manner, bare ITO electrode was covered with graphite-like carbon nitride (g-C₃N₄)–AuNPs nano hybrids for sensing of PKA.¹¹⁰ The peptide substrate and Phos-tag were immobilized onto the electrode successively. When the PKA concentration was increased from 0.05 to 100 units/mL, the photocurrent was enhanced gradually. This photoelectrochemical biosensor showed a detection limit of 15 U·L⁻¹ for PKA. The IC_{50} value of the model inhibitor HA-1077 was determined to be 1.18 μ M.

Disadvantages of Photoelectrochemical Biosensors. In fact, limitation is also associated with PEC biosensor. For instance, the common photoactive species are subject to susceptibilities to photobleaching and low photo-to-current conversion efficiencies. Meanwhile, the established signaling mechanisms are still highly restricted. Implementing these protocols in real-world applications is still a challenge.

DESIGN OF BIOSENSORS FOR DRUG EFFICACY ASSESSMENT AND TOXICITY EVALUATION

Efficacy assessment plays a prerequisite role in discovering sophisticated drugs. Numerous cell models or animal models can be used for it, such as small transgenic rodents and large animals with multiple diseases.¹¹³ The purpose of efficacy evaluation for potential candidates in animal models is to confirm the anticipated mechanism of action through the defined biomarkers and to lay a foundation for commencing studies in patients with related diseases.

The evaluation of drug-induced toxicity also represents a tricky challenge in drug development. For instance, hepatotoxicity is considered as the major cause for the FDA refusing to pass the drugs or withdrawing them from the market after approval.¹¹⁴ Toxicology evaluation has been relocated into the drug discovery phase. Innovative biosensors can reduce toxicity in the process of drug development. Biosensors can be tailored to respond to specific biomarkers or molecular events and then change their signals.

Förster Resonance Energy Transfer Biosensors. FRET biosensors have been designed for the evaluation of drug efficacy or toxicity in living cells and in vivo. For example, in order to evaluate the efficacy of an anticancer drug in a transgenic p53 mutant mouse model of pancreatic cancer, Nobis and co-workers¹¹⁵ developed a fluorescence lifetime imaging microscopy–fluorescence resonance energy transfer (FLIM-FRET) Src biosensor, which is comprised of ECFP and YPet as FRET donor and acceptor. Observed by the FRET biosensor, Src activity turns back immediately to a manageable level when applying post-dasatinib within 4–6 h. This research indicates the partially ineffective drug targeting against pancreatic tumors. This project highlights the potential application of FLIM-FRET for evaluating the efficacy of an anticancer drug.

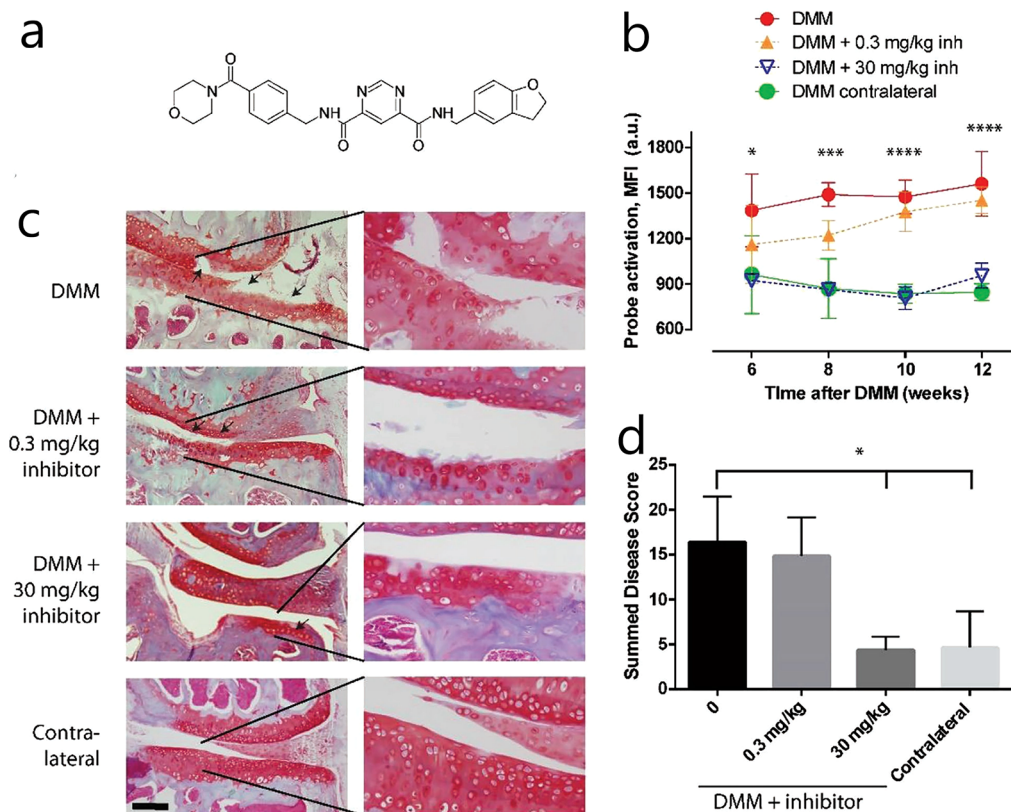


Figure 4. In vivo evaluation of the efficacy of MMP-13 inhibitor A4727 in the OA model. (a) Chemical structure of MMP-13 inhibitor A4727. (b) Activation of the PGA-P-18 probe after the DMM surgery in the knees of mice receiving no inhibitor (DMM and DMM contralateral) and a suboptimal dose ($0.3 \text{ mg}\cdot\text{kg}^{-1}$) and an optimal dose of MMP-13 inhibitor A4727 ($30 \text{ mg}\cdot\text{kg}^{-1}$). (c) Representative histology of the damage observed in the mouse knee joints at 12 weeks after the DMM surgery: DMM, surgery only; DMM + inhibit, DMM surgery treated with daily dose of MMP-13 inhibitor A4727; contralateral, contralateral knee of the mice treated with $30 \text{ mg}\cdot\text{kg}^{-1}$ inhibitor. Black arrows indicate areas of aggrecan degradation. (d) Summed disease scores as determined by histology at 12 weeks after DMM surgery. Reprinted with permission from ref 123. Copyright 2018 John Wiley and Sons.

Evaluating a drug candidate in preclinical animal models is an expensive and time-consuming process. Research on the relationship between cell models and animal models has gained increasing attention. For instance, Gómez-Soler and co-workers¹¹⁶ developed a kind of FRET biosensor in cells for predicting the anti-nociceptive efficacy of $\sigma 1$ receptor ligands in mouse. CFP and YFP are genetically fused to the N- and C-terminal domains of the receptor, serving as the donor and acceptor of FRET. The result of the FRET biosensor in cells was consistent with that of the traditional formalin test in mouse, showing the ability of the biosensor for predicting the intrinsic analgesic nature of $\sigma 1$ receptor ligands. Moreover, Kondo and co-workers^{117–119} made an improved FRET-based biosensor. It can efficiently quantify the kinase activity of BCR-ABL from patients' bone marrow cells and evaluate the inhibitory activity of tyrosine kinase inhibitors (TKIs) against BCR-ABL. Fluorescent proteins CFP and YFP function as the FRET donor and acceptor, respectively. This FRET-based biosensor shows the capability to predict the efficacy of dasatinib and nilotinib for treating patients with chronic myeloid leukemia (CML).

Mitochondrial toxicity is regarded as the main source of preclinical drug attrition, black box warning, and postmarket drug withdrawal. Contreras-Baeza and co-workers¹²⁰ have developed a genetically encoded FRET biosensor, i.e. Laconic, for mitochondrial toxicity assessment. The accumulation of cytosolic lactate induced by mitochondrial damage could be

measured by using the biosensor. A cancer cell line MDA-MB-231 that stably expresses Laconic is generated for the detection of mentioned toxic drugs in a 96-well format.

Advantages of Förster Resonance Energy Transfer Biosensors. FRET biosensors own the merits of high sensitivity, specificity, and fast responsibility. The light and homogeneous FRET biosensor will facilitate accurate quantitative measurement in vitro and in living cells.

Disadvantages of Förster Resonance Energy Transfer Biosensors. Despite the wide range of applications, FRET biosensors are still facing severe challenges such as high-resolution of fluorescent signals, the affordability of FRET reagents, and the specificity of the reaction.

Time-Resolved Förster Resonance Energy Transfer Biosensors. TR-FRET biosensor has been designed for drug efficacy assessment in cells. For instance, human epidermal growth factor receptor (HER) heterodimers are implicated in cancer cell resistance to various anticancer drugs. In order to detect efficacy of drug targeting EGFR/HER2 heterodimers in ovarian carcinoma cell line (SKOV-3) and compare with their efficacy in xenografted nude mice, Gaborit and co-workers¹²¹ fabricated an antibody-based TR-FRET biosensor. Terbium cryptate was selected as long-lived fluorescence donor, and the d2 dye was selected as an acceptor. Besides, the effect of different targeted therapies including trastuzumab, pertuzumab, and cetuximab on EGFR/HER2 dimers was assessed in SKOV-3 cells and SKOV-3 xenografted mice. The result

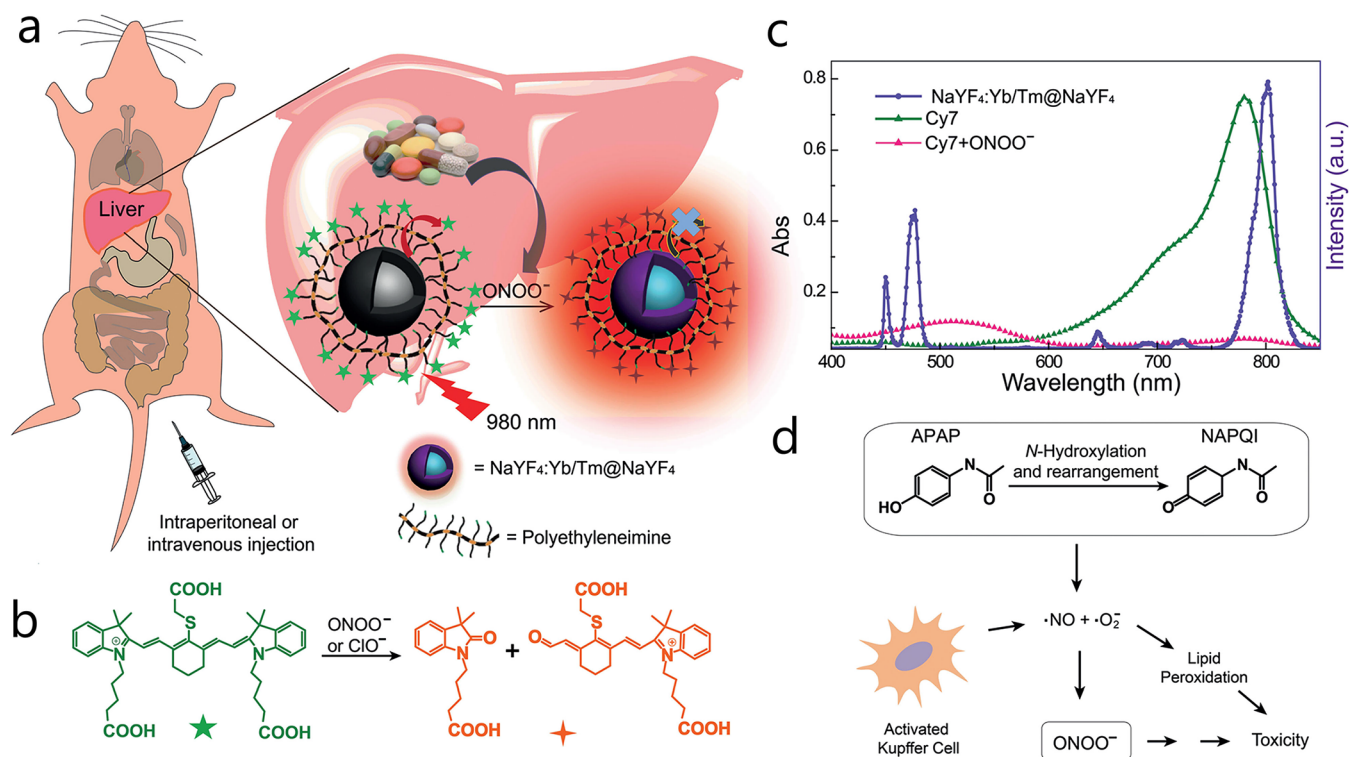


Figure 5. NIR biosensor for evaluation drug-induced hepatotoxicity. (a) Rational design of chromophore-assembled UCNPs for the detection of nitrosative hepatotoxicity in vivo. (b) Proposed reaction mechanism for the “turn-on” luminescence by which the energy acceptor Cy7 (marked with green star) degrades after oxidation by ONOO^- or ClO^- . (c) UV/vis spectra of chromophore measured in the absence (green line, 28 mM) and presence (red line, 18 mM) of ONOO^- and up-conversion emission spectra of UCNPs under excitation at 980 nm (purple line). (d) Mechanism of APAP-induced hepatotoxicity. Reprinted with permission from ref 125. Copyright 2017 John Wiley and Sons.

showed that the monoclonal antibody (mAb) therapeutic effect in SKOV-3 xenografted mice was correlated well with their efficiency in decreasing the concentration of EGFR/HER2 heterodimers in SKOV-3 cells. This work provides an antibody-based TR-FRET biosensor, which serves as a useful method for predicting the efficacy of mAbs targeting EGFR/HER2 heterodimers.

Advantages of Time-Resolved Förster Resonance Energy Transfer Biosensors. TR-FRET biosensors owned various advantages. First, TR-FRET biosensor has a high sensitivity and wide linear range (pg/mL to $\mu\text{g/mL}$). Second, the operation procedure of TR-FRET biosensor is simple, time-saving, and labor-saving. There is no need to coat or wash the plate. Third, there is no significant decrease in fluorescence signal >48 h, and no photobleaching phenomenon.

Disadvantages of Time-Resolved Förster Resonance Energy Transfer Biosensors. The shortcomings of TR-FRET have been described before in the drug screening section.

Aggregation-Induced Emission Biosensors. AIE biosensors are currently used for drug efficacy assessment or toxicity evaluation in cells. For instance, the clinical use of platinum drug is still limited due to the severe side effects. In order to non-invasively early evaluate platinum drug's therapeutic responses in situ and reduce its side effects, Yuan and co-workers⁶⁹ designed a Pt(IV) prodrug which was composed of an apoptosis biosensor (TPS-DEVD) with AIE characteristics and a cyclic (RGD) peptide. The Pt(IV) prodrug was reduced to the active Pt(II) in cells, which further triggered the apoptosis of the cancer cell and activated the caspase-3. The cleavage of the DEVD sequence of the

apoptosis biosensor led to the AIE effect of TPS residue. The AIE biosensor allowed one to evaluate the drug therapeutic response in cells quickly.

Advantages of Aggregation-Induced Emission Biosensors. The advantages of AIE biosensors are apparent. First, they exhibit strong stability to ultraviolet excitation light (no photobleaching). Second, they have strong luminescence characteristics in solid state (powder or high concentration). Third, they can be utilized in cell imaging and related biological imaging, which produces high-resolution images. Fourth, the higher the concentration, the stronger the luminescence of AIE biosensor. Last but not the least important, flexible chemical modification of AIE biosensor can be used to achieve different wavelengths of luminescence control.

Disadvantages of Aggregation-Induced Emission Biosensors. In vivo applications require low autofluorescence and deep penetration. Nevertheless, most AIE biosensors utilized shorter wavelength emissive AIE probes such as blue or green, which have limited the further practical applications in vivo. In order to expand the scope of their applications in vivo, one alternative strategy is to create far-red/near-infrared fluorescent AIE biosensors with multiple functionalities.

Near-Infrared Fluorescence Biosensors. Near-infrared fluorescence biosensor in the first near-infrared window (NIR-I, 650–900 nm) owns the merits of little biological autofluorescence and low photodamage, which are desirable for practical applications in drug efficacy assessment in live animals.¹²² An enzyme activatable NIR-based peptide biosensor called PGA-P-18, which comprised a biphenyl triazole, a NIR group Cy5.5, and a quencher group QSY21, was

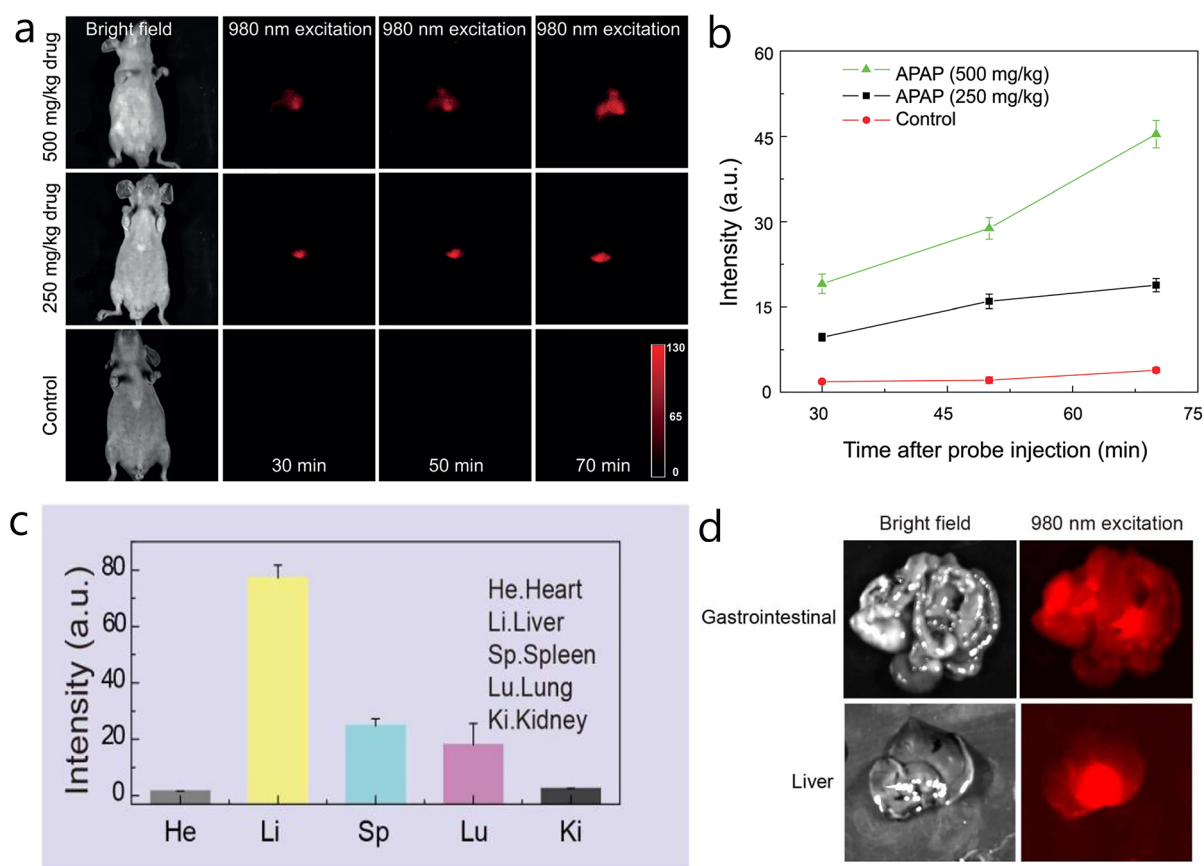


Figure 6. Representative images of mice receiving NIR nanoprobes after drug treatment. (a) Mice receiving nanoprobes pretreated with 500 and 250 mg·kg⁻¹ paracetamol or PBS buffer (control) at different time points. The images were collected at 790 ± 40 nm upon irradiation at 980 nm. (b) The luminescence intensity over time. Data were obtained from the liver area of the images after the background was subtracted (*n* = 3 mice per group). Reprinted with permission from ref 125. Copyright 2017 John Wiley and Sons.

synthesized and employed for evaluating the efficacy of a matrix metalloproteinase 13 (MMP-13) inhibitor, i.e., A4727 (see Figure 4a) in a mouse model of osteoarthritis.¹²³ It is worth noting that the biosensor shows high specificity toward MMP-13 and can distinguish between osteoarthritic knees and sham-operated knees. As is shown in Figure 4b, MMP-13 activity was completely blocked by oral administration of A4727 at routine dosage (30 mg/kg). Histological analysis of the knees at 12 weeks revealed that the degree of cartilage protection was consistent with the blockade of the MMP-13 activity (see Figure 4c,d). This work provided a useful NIR biosensor for evaluation the anti-osteoarthritis efficacy of potential candidates.

Oxidative stress and cellular apoptosis are observed to be increased at the early stage of hepatotoxicity and nephrotoxicity. Thus, a series of NIR biosensors have been developed for monitoring biomarkers of oxidative stress and cellular apoptosis, providing evidence for drug-induced hepatotoxicity^{124–129} and nephrotoxicity.^{130–132} As a typical example, lanthanide-doped UCNP were successively functionalized with PEI and Cy7 chromophore (see Figure 5a). The core-shell UCNP served as an energy donor, while the Cy7 chromophore acted as an energy acceptor. Upon reacting with ONOO⁻, the Cy7 chromophore was degraded (see Figure 5b) and the biosensor generated NIR emission at 800 nm (see Figure 5c). ONOO⁻ was produced in the liver tissue after administration of overdose paracetamol to rats (see Figure 5d). When the time increased from 30 to 70 min, a remarkable

enhancement of luminescent signals was observed in the liver region (see Figure 6a). Meanwhile, the intensity of the signals was dose-dependent (see Figure 6b). Compared with heart, spleen, lung, and kidney, the biosensor showed high specificity for the liver tissue (see Figure 6c). This work provided a useful biosensor for evaluation of hepatotoxicity of synthetic drugs. However, the luminescence signal was also observed for the gastrointestinal tract (see Figure 6d). The potential of NIR biosensor for evaluating the intestinal epithelial toxicity needs to be clarified.

Advantages of Near-Infrared Fluorescence Biosensors. Traditional methods always sacrificed the model animals at various time points. The evaluation of the potential candidates was carried out on different animals, which would introduce individual variations. In contrast, NIR biosensors provided an *in vivo* and real-time approach to acquire the spatiotemporal distribution and pharmacodynamics information on potential candidates. No sacrifice of the animals was required. Therefore, individual differences were eliminated. Imaging at the NIR-I window in live animals is regarded as the gold standard in the past few years. Moreover, NIR biosensor at the second near-infrared window (NIR-II, 1000–1700 nm) owns superior sensitivity and resolution over NIR-I *in vivo*,¹³³ which will pave the way for highly efficient potential candidates assessment at the model-animal level and will facilitate the translation of potential candidates to clinical practices.

Disadvantages of Near-Infrared Fluorescence Biosensors. NIR-I fluorescence biosensors suffered from the light

absorption and scattering of tissues, leading to significant attenuation of excitation light, poor signal-to-background ratio, and low sensitivity.¹³⁴ Thus, NIR-I fluorescence biosensors is not amenable to deep-tissue imaging. Meanwhile, most NIR-II imaging agents are inorganic nanoparticles which can be easily adjusted to the NIR-II window. However, optical properties, biodistribution, and kinetics of inorganic nanoparticles are difficult to control to fulfill the requirements of efficacy assessment. Therefore, the development of more effective NIR-II nanoparticles¹³⁵ or organic semiconducting agents¹³⁶ for NIR-II imaging will increase their potential for clinical translation.

DESIGN OF HYBRID BIOSENSORS

FRET and CRET Hybrid Biosensors. Hybrid biosensors have attracted a growing amount of attention, since they can detect more than one biomarker or target simultaneously (see Table S11). For instance, the aforementioned NIR biosensors can only monitor one biomarker of hepatotoxicity such as ONOO⁻. However, ROS always occurs before the formation of ONOO⁻ in the process of hepatotoxicity. Subsequently, hybrid FRET and CRET biosensors called CF-SPNs are created.¹²⁴ The hybrid biosensors comprise four functional parts, including a NIR semiconducting polymer PFODBT, a galactosylated graft copolymer, a cyanine dye (IR775S), and a hydrophobic peroxyoxalate (CPPO). The hybrid biosensors are applied to the imaging of both ROS and RNS. PFODBT and IR775S served as energy donor and energy acceptor, respectively. In the presence of H₂O₂, peroxyoxalate is decomposed to 1, 2-dioxatanedione, which is able to induce the chemiluminescence. If ONOO⁻ or ⁻OCl is generated in the liver, the degradation of IR775S causes a shutdown of the FRET signal. The average diameters of the spherical CF-SPNs particles are around 50 nm. Hybrid biosensors are employed to detect isoniazid (INH)-induced hepatotoxicity in vivo. The most intensive level of luminescence is observed at 10 min after INH administration, while the largest fluorescence index is reached at 70 min. The degree of hepatocyte vacuolization was closely correlated with the dose of INH. The trend of NIR imaging is remarkably consistent with that of H&E staining. This project confirms the effects of hybrid biosensors in monitoring drug-induced hepatotoxicity in vivo.

Chemo-fluoroluminescent Hybrid Biosensors. An unimolecular chemo-fluoroluminescent hybrid biosensor, called chemo-fluoroluminescent reporter (CFR), is created for duplex imaging of drug-induced hepatotoxicity.¹²⁸ The hybrid biosensor can detect the activity of O₂^{•-} and caspase-3 at the same time through chemiluminescence and NIR channels. Strikingly, CFR can observe hepatotoxicity induced by anti-epileptic drug valproic acid in the first 17.5 h of histological changes. Such a molecular design of CFR can be adapted for duplex imaging of other biomarkers by making some tweaks of the caging groups on both chemiluminescence and NIR signaling moieties.

The main barrier of monitoring nephrotoxicity is the development of biosensors with strong signal-to-background ratio and high rate of renal clearance. One group works on developing chemo-fluoroluminescent hybrid biosensors for evaluation of drug-induced nephrotoxicity.¹³⁰ There are three biomarkers that include O₂^{•-}, NAG, and caspase-3. They can represent different stages of acute kidney injury. MRP1–3 biosensors switch on their fluorescence as their respective biomarkers were available. After reaction with O₂^{•-}, MRP_D

biosensor becomes chemiluminescent. What is interesting is that both MRP1 and MRP_D biosensors are designed for sensing O₂^{•-}. The fluorescence results of MRP1, MRP2, and MRP3 are shown respectively in kidney at 12, 16, and 48 h after treatment with cisplatin. Confocal fluorescence microscopy images of slices in an entire kidney from mice suggest that the deterioration of the kidney spreads from the renal cortex to the medullin, which matched well with the trend of NIR imaging data. Compared with traditional clinical indicators of nephrotoxicity (i.e., creatinine and blood urea nitrogen), this MRP chemo-fluoroluminescent hybrid biosensor shows overwhelming advantages and can detect nephrotoxicity more than 30 hours earlier than using conventional methods.

FRET and AIE Hybrid Biosensors. In addition to evaluating toxicity, hybrid biosensors can also be used for drug efficacy assessment. For instance, Wang and co-workers¹³⁷ develop a doxorubicin-loaded biosensor, where the AIE luminogen TPE-CHO works as a FRET donor for antitumor drug doxorubicin. They succeed in assessing the efficacy of doxorubicin in A549 cells by using the AIE and FRET hybrid biosensor. Furthermore, by taking the hyperbranched polyamide amine (H-PAMAM) with intrinsic AIE effects as the core and taking advantage of FRET effects between H-PAMAM and doxorubicin (DOX), the hybrid biosensor is fabricated in another project.¹³⁸ The study of vitro cytotoxicity in MCF-7 cells shows that the DOX-loaded biosensor had a promising therapeutic effect on cancer.

CONCLUSION AND PERSPECTIVE

From the perspective of biosensors, the detection limit and dynamic range of a biosensor are critical parameters to be taken into consideration. To lower the detection limit and increase the dynamic range are generally the purpose of biosensor optimization. The dynamic range of the biosensors can be extended by switching fluorophores, improving linkers, and enhancing targets binding to the biosensor. The majority of biosensors, including surface plasmon resonance, fluorescent, photoelectrochemical, and electrochemical systems, have been developed for the procedure in the lead generation step of the drug discovery pipeline. As to drug discovery, ease of automation, high precision, and high-throughput are of great importance. Fluorescent biosensor still dominated the preliminary lead generation step due to its excellent performance in the field. Meanwhile, surface plasmon resonance biosensor maintains the most authoritative standard on studying drug–target interaction, which may be suitable for secondary screening against a small library of compounds due to its high cost. Besides, photoelectrochemical and electrochemical biosensors could be an effective supplement to fluorescent methods for preliminary screening if the biosensors are adjusted and tuned to fit for the screening paradigm. It is encouraging that great endeavors have been made in establishing NIR biosensors to evaluate potential candidate-induced toxicity. Nevertheless, the biosensors for evaluating the efficacy of potential candidate are still very rare, which points to the need for further exploration and efficient efforts.

Fusion of Biosensors Based on Different Mechanism. The specificity of a potential candidate toward a target is crucial to drug discovery. In other words, the “off-target” effect needs to be prudently evaluated at the onset of drug discovery. A single-mechanism-based biosensor only accomplishes drug screening against one target, which is apparently insufficient. Multifunctional biosensors such as FRET with AIE or

fluorescence with chemiluminescence will make the biosensor more versatile and even suitable for realization of multiple targets evaluation in only one test, which will speed up the drug discovery process and cut the cost.

Drug Target Selection of Higher Validity. As indicated in an investigation, successful drug discovery projects concentrated on a limited set of well-validated therapeutic mechanisms–indications pair, while failure rates of drug discovery in phase II or III trials interrupted by efficacy issues were around ~50–60% between 2008 and 2015,¹³⁹ which revealed that effective target selection plays a pivotal role in drug R&D. Improved efficacy or low price bring about a bright prospect for drugs of the second generation or the congeneric. However, current drug discovery pipelines are more interested in innovative mechanisms, the rigorous validation of which takes time.

Efficacy Evaluation on 3D Organoids. It is necessary to re-evaluate the predictive power of such animal models as drug failures in clinical trials are primarily due to the lack of translatability from strong therapeutic evidence in animal models into human disease therapeutics. In this context, human-derived organoids have emerged as stable preclinical models for efficacy assessment. A representative example is the human pluripotent stem cells (hPSCs) lung-derived organoid model. Three SARS-CoV-2 inhibitors, including imatinib, mycophenolic acid, and quinacrine dihydrochloride,¹⁴⁰ were successfully identified under this organoid model. These inhibitors could significantly inhibit SARS-CoV-2 infection. In addition, patient-derived cancer organoids can recapitulate patient responses in the clinic.¹⁴¹ Integrating these human organoid models with microfluidic chips is superior for in vitro cell culture models and animal models.¹⁴² The organ-on-a-chip technology will realize its full potential when applied into commercial drug discovery in the future.

■ ASSOCIATED CONTENT

SI Supporting Information

The Supporting Information is available free of charge at <https://pubs.acs.org/doi/10.1021/acssensors.1c01600>.

(Table S1) Strengths and limitations of current biosensors; (Table S2) SPR biosensor key examples; (Table S3) optical waveguide grating biosensor selected cases; (Table S4) biolayer interferometry biosensors; (Table S5) grating coupled interferometry biosensor recent applications; (Table S6) several important FRET biosensors; (Table S7) AIE biosensor representative examples; (Table S8) other fluorescent biosensors; (Table S9) electrochemical biosensors; (Table S10) photoelectrochemical biosensors; (Table S11) hybrid biosensors (PDF)

■ AUTHOR INFORMATION

Corresponding Authors

Yi Tao – College of Pharmaceutical Science, Zhejiang University of Technology, Hangzhou 310014, China; orcid.org/0000-0002-1593-2738; Phone: 86-025-86798281; Email: taoyi1985@zjut.edu.cn; Fax: 86-025-86798281

Dong Zhu – School of Pharmacy, Nanjing University of Chinese Medicine, Nanjing, Jiangsu 210023, China; orcid.org/0000-0002-7365-5556; Email: dongzhu@njucm.edu.cn

Authors

Lin Chen – College of Pharmaceutical Science, Zhejiang University of Technology, Hangzhou 310014, China
Meiling Pan – College of Pharmaceutical Science, Zhejiang University of Technology, Hangzhou 310014, China
Fei Zhu – College of Pharmaceutical Science, Zhejiang University of Technology, Hangzhou 310014, China

Complete contact information is available at:
<https://pubs.acs.org/10.1021/acssensors.1c01600>

Notes

The authors declare no competing financial interest.

■ ACKNOWLEDGMENTS

This work was granted funding by the National Natural Science Foundation of China (No. 81703701), Natural Science Foundation of Zhejiang Province (No. Y21H280036), Postdoctoral Science Foundation funded project of Zhejiang Province (No. 228194), and Youth Talent Cultivation Project of Zhejiang Association for Science and Technology (No. KYY-ZX-20200170). We thank the anonymous reviewers for their invaluable suggestions that helped improve the manuscript.

■ ABBREVIATIONS

ACE, angiotensin converting enzyme; AChE, acetylcholinesterase; ACQ, aggregation-caused quenching; AgNCs, silver nanoclusters; AIE, aggregation-induced emission; ALDH, aldehyde dehydrogenases; AMC, 7-amino-4-methylcoumarin; APAP, acetaminophen; AuNCs, gold nanocluster; AuNPs, gold nanoparticles; BLI, biolayer interferometry; BODIPY, 4,4-difluoro-4-bora-3a,4a-diaza-s-indacene; CBP BrD, cAMP-responsive element binding protein binding protein bromodomain; CDs, carbon dots; CFP, cyan fluorescent protein; CFR, chemo-fluoroluminescent reporter; CML, chronic myeloid leukemia; ColH, collagenase H; CPPO, hydrophobic peroxalate; CRET, chemiluminescence resonance energy transfer; CXCR4, C-X-C motif chemokine receptor 4; Cy7, cyanine7; DNA MTases, DNA methyltransferase; DOX, doxorubicin; DPP-4, dipeptidyl peptidase-4; DV RdRp, Dengue virus RNA-dependent RNA polymerase; ECFP, cyan fluorescence protein; EDC, 1-ethyl-3-(3-(dimethylamino)propyl)carbodiimide; EGFR, epidermal growth factor receptor; ENPP1, ectonucleotide pyrophosphatase/phosphodiesterase 1; ER, estrogen receptor; FALGPA, FA-LEU-GLY-PRO-ALA-OH; FAP α , fibroblast activation protein; FDA, U.S. Food and Drug Administration; FLIM-FRET, fluorescence lifetime imaging microscopy–fluorescence resonance energy transfer; FRET, Förster resonance energy transfer; GABA_A receptor, γ -aminobutyric acid A receptor; GABA_B receptor, γ -aminobutyric acid B receptor; GBZ, guanabenz; GGT, γ -glutamyl transpeptidase; GLS1, glutaminase; GPCRs, G-protein-coupled receptors; hACE2, human angiotensin converting enzyme 2; HAT, histone acetyltransferases; HDACs, histone deacetylases; HER, human epidermal growth factor receptor; HIV-1 RT, reverse transcriptase of human immunodeficiency virus 1; hNTH1-YB1, human endonuclease-Y-box binding protein 1; H-PAMAM, hyperbranched polyamide amine; HPS, hexaphenylsilole; hPSC, human pluripotent stem cells; HTS, high-throughput screening; INH, isoniazid; IR, insulin receptors; ITO, indium tin oxide; KD, dissociation constants; LANCL2, LanC lantibiotic synthetase component C-like 2;

LH, luteinizing hormone receptor; mAb, monoclonal antibody; MCH, 6-mercapto-1-hexanol; mGlu, metabotropic glutamate receptors; mGlu 2, metabotropic glutamate receptor 2; MMPs, matrix metalloproteinases; MMP-13, matrix metalloproteinase 13; MRP, molecular renal probes; 11-MUA, 11-mercaptopoundecanoic acid; NHS, *N*-hydroxysuccinimide; Ni-NTA, nickel agarose; NIR, near-infrared; NIRF, near-infrared fluorescence biosensor; OWG, optical waveguide grating; PARP, poly(ADP-ribose) polymerase; PEC, photoelectrochemical biosensors; PEI, polyethylenimine; PET, photoinduced electron transfer; PGA, penicillin G acylase; PI3K γ , PI-3 kinase gamma; PKA, protein kinase A; PPIc, protein phosphatase 1 catalytic subunit; PTH, class B parathyroid hormone receptor 1; PTP1B, protein tyrosine phosphatase 1B; QDs, quantum dots; QRET, quenching resonance energy transfer; R15A, protein phosphatase 1 regulatory subunit 15A; RIR, intramolecular rotations; RIV, intramolecular vibration; RNase H, ribonuclease H; ROS, reactive oxygen species; RT, reverse transcriptase; RTKs, receptor tyrosine kinases; SARSCoV-2 RBD, SARS-CoV-2 spike receptor binding domain; S/B, signal/background; SERCA2a-PLB, sarco/endoplasmic reticulum Ca²⁺-ATPase-phospholamban; SPR, surface plasmon resonance; Src, sarcoma gene; STAT3, signal transducer and activator of transcription 3; TCh, thiocholine; THBA, 10,10',11,11'-tetrahydro-5,5'-bidibenzo[*a,d*][7]-annulenyliene; TKI, tyrosine kinase inhibitors; TNF, tumor necrosis factor; TPA, triphenylamine; TPE, tetraphenylethylene; TPETH, tetraphenylethylene-thiophene; TPS, tetraphenylsilole; TR-FRET, time-resolved Förster resonance energy transfer; TYR, tyrosinase; T4 PNK, T4 polynucleotide kinase; UCNPs, up-conversion nanoparticles; VIM-2, Verona integron-encoded metallo- β -lactamase; YFP, yellow fluorescent protein; YPet, yellow fluorescent protein for energy transfer

VOCABULARY

Surface plasmon resonance biosensor, Surface plasmon resonance biosensor is a golden standard for studying drug–target interactions and providing a huge stage for drug screening; Optical waveguide grating biosensor, Optical waveguide grating biosensor takes advantage of resonant waveguide gratings or nanostructured optical gratings to identify binders of target proteins; Biolayer interferometry biosensor, Biolayer interferometry biosensor analyzes the interference pattern of white light reflected from a layer of immobilized drug targets on the tip of a biosensor against an internal reference; Switchsense biosensor, Switchsense biosensor monitors the changes in hydrodynamic friction of the DNA nanolever on the gold surface, which can be affected by the binding of compounds to drug targets; Förster resonance energy transfer biosensor, Förster resonance energy transfer biosensor is a process of nonradioactive energy transfer between the donor–acceptor pairs; Aggregation-induced emission biosensor, Aggregation-induced emission biosensor is non-emissive when molecularly dissolved in solution but induced to emit efficiently by aggregation; Photoelectrochemical biosensor, A photoelectrochemical biosensor consists of an excitation source, a cell, and an electrochemical workstation with a three-electrode system.

REFERENCES

- (1) Schneider, G. Automating drug discovery. *Nat. Rev. Drug Discovery* **2018**, *17*, 97–113.
- (2) Renaud, J.; Chung, C.; Danielson, U. H.; Egner, U.; Hennig, M.; Hubbard, R. E.; Nar, H. Biophysics in drug discovery: impact, challenges and opportunities. *Nat. Rev. Drug Discovery* **2016**, *15*, 679–698.
- (3) Yang, X.; Wang, Y.; Byrne, R.; Schneider, G.; Yang, S. Concepts of Artificial Intelligence for Computer-Assisted Drug Discovery. *Chem. Rev.* **2019**, *119*, 10520–10594.
- (4) Wu, Y.; Tilley, R. D.; Gooding, J. J. Challenges and Solutions in Developing Ultrasensitive Biosensors. *J. Am. Chem. Soc.* **2019**, *141*, 1162–1170.
- (5) Wongkaew, N.; Simsek, M.; Griesche, C.; Baeumner, A. J. Functional Nanomaterials and Nanostructures Enhancing Electrochemical Biosensors and Lab-on-a-Chip Performances: Recent Progress, Applications, and Future Perspective. *Chem. Rev.* **2019**, *119*, 120–194.
- (6) Scott, D. E.; Bayly, A. R.; Abell, C.; Skidmore, J. Small molecules, big targets: drug discovery faces the protein–protein interaction challenge. *Nat. Rev. Drug Discovery* **2016**, *15*, 533–550.
- (7) Cooper, M. A. Optical biosensors in drug discovery. *Nat. Rev. Drug Discovery* **2002**, *1*, 515–528.
- (8) Halai, R.; Cooper, M. A. Using label-free screening technology to improve efficiency in drug discovery. *Expert Opin. Drug Discovery* **2012**, *7*, 123–131.
- (9) Cooper, M. A. Optical biosensors: where next and how soon? *Drug Discovery Today* **2006**, *11*, 1061–1067.
- (10) Christopheit, T.; Carlsen, T. J. O.; Helland, R.; Leiros, H.-K. S. Discovery of Novel Inhibitor Scaffolds against the Metallo- β -lactamase VIM-2 by Surface Plasmon Resonance (SPR) Based Fragment Screening. *J. Med. Chem.* **2015**, *58*, 8671–8682.
- (11) Schönauer, E.; Kany, A. M.; Hauptenthal, J.; Hüsecken, K.; Hoppe, I. J.; Voos, K.; Yahiaoui, S.; Elsässer, B.; Ducho, C.; Brandstetter, H.; Hartmann, R. W. Discovery of a Potent Inhibitor Class with High Selectivity toward Clostridial Collagenases. *J. Am. Chem. Soc.* **2017**, *139*, 12696–12703.
- (12) Cao, Y.; Li, Y.; Lv, D.; Chen, X.; Chen, L.; Zhu, Z.; Chai, Y.; Zhang, J. Identification of a ligand for tumor necrosis factor receptor from Chinese herbs by combination of surface plasmon resonance biosensor and UPLC-MS. *Anal. Bioanal. Chem.* **2016**, *408*, 5359–5367.
- (13) Chen, L.; Lv, D.; Chen, X.; Liu, M.; Wang, D.; Liu, Y.; Hong, Z.; Zhu, Z.; Hu, X.; Cao, Y.; Yang, J.; Chai, Y. Biosensor-based active ingredients recognition system for screening STAT3 ligands from medicinal herbs. *Anal. Chem.* **2018**, *90*, 8936–8945.
- (14) Chen, L.; Lv, D.; Wang, S.; Wang, D.; Chen, X.; Liu, Y.; Hong, Z.; Zhu, Z.; Cao, Y.; Chai, Y. Surface Plasmon Resonance-Based Membrane Protein-Targeted Active Ingredients Recognition Strategy: Construction and Implementation in Ligand Screening from Herbal Medicines. *Anal. Chem.* **2020**, *92*, 3972–3980.
- (15) Kong, W.; Wu, D.; Hu, N.; Li, N.; Dai, C.; Chen, X.; Suo, Y.; Li, G.; Wu, Y. Robust hybrid enzyme nanoreactor mediated plasmonic sensing strategy for ultrasensitive screening of anti-diabetic drug. *Biosens. Bioelectron.* **2018**, *99*, 653–659.
- (16) Zhou, W.; Yang, M.; Li, S.; Zhu, J. Surface plasmon resonance imaging validation of small molecule drugs binding on target protein microarrays. *Appl. Surf. Sci.* **2018**, *450*, 328–335.
- (17) Krzyzosiak, A.; Sigurdardottir, A.; Luh, L.; Carrara, M.; Das, I.; Schneider, K.; Bertolotti, A. Target-based discovery of an inhibitor of the regulatory phosphatase PPP1R15B. *Cell* **2018**, *174*, 1216–1228.
- (18) Gangadhara, G.; Dahl, G.; Bohnacker, T.; Rae, R.; Gunnarsson, J.; Blaho, S.; Öster, L.; Lindmark, H.; Karabelas, K.; Pemberton, N.; Tyrchan, C.; Mogemark, M.; Wymann, M. P.; Williams, R. L.; Perry, M. W. D.; Papavoine, T.; Petersen, J. A class of highly selective inhibitors bind to an active state of PI3K γ . *Nat. Chem. Biol.* **2019**, *15*, 348–357.
- (19) Tao, Y.; Chen, L.; Jiang, E. Layer-by-layer assembly strategy for fabrication of polydopamine-polyethylenimine hybrid modified fibers and their application to solid-phase microextraction of bioactive molecules from medicinal plant samples followed by surface plasmon

- resonance biosensor validation. *Anal. Chim. Acta* **2021**, *1146*, 155–165.
- (20) Xia, Y.; Wu, L.; Hu, Y.; He, Y.; Cao, Z.; Zhu, X.; Yi, X.; Wang, J. Sensitive surface plasmon resonance detection of methyltransferase activity and screening of its inhibitors amplified by p53 protein bound to methylation-specific ds-DNA consensus sites. *Biosens. Bioelectron.* **2019**, *126*, 269–274.
- (21) Cichero, E.; Fresia, C.; Guida, L.; Booz, V.; Millo, E.; Scotti, C.; Iamele, L.; de Jonge, H.; Galante, D.; De Flora, A.; Sturla, L.; Vigliarolo, T.; Zocchi, E.; Fossa, P. Identification of a high affinity binding site for abscisic acid on human lanthionine synthetase component C-like protein 2. *Int. J. Biochem. Cell Biol.* **2018**, *97*, 52–61.
- (22) Geschwindner, S.; Carlsson, J. F.; Knecht, W. Application of optical biosensors in small-molecule screening activities. *Sensors* **2012**, *12*, 4311–4323.
- (23) Deng, H.; Wang, C.; Su, M.; Fang, Y. Probing biochemical mechanisms of action of muscarinic M3 receptor antagonists with label-free whole cell assays. *Anal. Chem.* **2012**, *84*, 8232–8239.
- (24) Song, H.-P.; Wang, H.; Zhao, X.; He, L.; Zhong, H.; Wu, S.-Q.; Li, P.; Yang, H. Label-free pharmacological profiling based on dynamic mass redistribution for characterization and authentication of hazardous natural products. *J. Hazard. Mater.* **2017**, *333*, 265–274.
- (25) Krebs, K. M.; Pfeil, E. M.; Simon, K.; Grundmann, M.; Häberlein, F.; Bautista-Aguilera, O. M.; Gütschow, M.; Weaver, C. D.; Fleischmann, B. K.; Kostenis, E. Label-Free Whole Cell Biosensing for High-Throughput Discovery of Activators and Inhibitors Targeting G Protein-Activated Inwardly Rectifying Potassium Channels. *ACS omega* **2018**, *3*, 14814–14823.
- (26) Zhou, H.; Peng, X.; Hou, T.; Zhao, N.; Qiu, M.; Zhang, X.; Liang, X. Identification of novel phytocannabinoids from Ganoderma by label-free dynamic mass redistribution assay. *J. Ethnopharmacol.* **2020**, *246*, 112218.
- (27) Kaminski, T.; Gunnarsson, A.; Geschwindner, S. Harnessing the Versatility of Optical Biosensors for Target-Based Small-Molecule Drug Discovery. *ACS sensors* **2017**, *2*, 10–15.
- (28) Choy, C. J.; Berkman, C. E. A method to determine the mode of binding for GCPII inhibitors using bio-layer interferometry. *J. Enzyme Inhib. Med. Chem.* **2016**, *31*, 1690–1693.
- (29) Zhu, M.; Fang, J.; Zhang, J.; Zhang, Z.; Xie, J.; Yu, Y.; Ruan, J. J.; Chen, Z.; Hou, W.; Yang, G.; Su, W.; Ruan, B. H. Biomolecular Interaction Assays Identified Dual Inhibitors of Glutaminase and Glutamate Dehydrogenase That Disrupt Mitochondrial Function and Prevent Growth of Cancer Cells. *Anal. Chem.* **2017**, *89*, 1689–1696.
- (30) Overacker, R. D.; Plitzko, B.; Loesgen, S. Biolayer interferometry provides a robust method for detecting DNA binding small molecules in microbial extracts. *Anal. Bioanal. Chem.* **2021**, *413*, 1159–1171.
- (31) Sima, L. E.; Yakubov, B.; Zhang, S.; Condello, S.; Grigorescu, A. A.; Nwani, N. G.; Chen, L.; Schiltz, G. E.; Arvanitis, C.; Zhang, Z.-Y.; Matei, D. Small Molecules Target the Interaction between Tissue Transglutaminase and Fibronectin. *Mol. Cancer Ther.* **2019**, *18*, 1057–1068.
- (32) Yang, L. J.; Chen, R. H.; Hamdoun, S.; Coghi, P.; Ng, J. P. L.; Zhang, D. W.; Guo, X.; Xia, C.; Law, B. Y. K.; Wong, V. K. W. Corilagin prevents SARS-CoV-2 infection by targeting RBD-ACE2 binding. *Phytomedicine* **2021**, *87*, 153591.
- (33) Peter, B.; Saffics, A.; Kovacs, B.; Kurunczi, S.; Horvath, R. Oxidization increases the binding of EGCG to serum albumin revealed by kinetic data from label-free optical biosensor with reference channel. *Analyst* **2020**, *145*, 588–595.
- (34) Kartal, Ö.; Andres, F.; Lai, M. P.; Nehme, R.; Cottier, K. waveRAPID-A Robust Assay for High-Throughput Kinetic Screens with the Creoptix WAVEsystem. *SLAS Discovery* **2021**, *26*, 995–1003.
- (35) Knezevic, J.; Langer, A.; Hampel, P. A.; Kaiser, W.; Strasser, R.; Rant, U. Quantitation of Affinity, Avidity, and Binding Kinetics of Protein Analytes with a Dynamically Switchable Biosurface. *J. Am. Chem. Soc.* **2012**, *134*, 15225–15228.
- (36) Müller-Landau, H.; Varela, P. F. Standard operation procedure for switchSENSE DRX systems. *Eur. Biophys. J.* **2021**, *50*, 389–400.
- (37) Schiedel, M.; Daub, H.; Itzen, A.; Jung, M. Validation of the Slow Off-Kinetics of Sirtuin-Rearranging Ligands (SirReals) by Means of Label-Free Electrically Switchable Nanolever Technology. *ChemBioChem* **2020**, *21*, 1161–1166.
- (38) Algar, W. R.; Hildebrandt, N.; Vogel, S. S.; Medintz, I. L. FRET as a biomolecular research tool — understanding its potential while avoiding pitfalls. *Nat. Methods* **2019**, *16*, 815–829.
- (39) Zhang, X.; Hu, Y.; Yang, X.; Tang, Y.; Han, S.; Kang, A.; Deng, H.; Chi, Y.; Zhu, D.; Lu, Y. Förster resonance energy transfer (FRET)-based biosensors for biological applications. *Biosens. Bioelectron.* **2019**, *138*, 111314.
- (40) Sun, J.; Yang, X. Gold nanoclusters—Cu²⁺ ensemble-based fluorescence turn-on and real-time assay for acetylcholinesterase activity and inhibitor screening. *Biosens. Bioelectron.* **2015**, *74*, 177–182.
- (41) Liu, J.-W.; Wang, Y.-M.; Xu, L.; Duan, L.-Y.; Tang, H.; Yu, R.-Q.; Jiang, J.-H. Melanin-like nanoquencher on graphitic carbon nitride nanosheets for tyrosinase activity and inhibitor assay. *Anal. Chem.* **2016**, *88*, 8355–8358.
- (42) Chen, J.; Wei, X.; Tang, H.; Ali, M. C.; Han, Y.; Li, Z.; Qiu, H. Highly discriminative fluorometric sensor based on luminescent covalent organic nanospheres for tyrosinase activity monitoring and inhibitor screening. *Sens. Actuators, B* **2020**, *305*, 127386.
- (43) Sharma, K. K.; Przybilla, F.; Restle, T.; Godet, J.; Mély, Y. FRET-based assay to screen inhibitors of HIV-1 reverse transcriptase and nucleocapsid protein. *Nucleic Acids Res.* **2016**, *44*, e74–e74.
- (44) Li, G.; Kong, W.; Zhao, M.; Lu, S.; Gong, P.; Chen, G.; Xia, L.; Wang, H.; You, J.; Wu, Y. A fluorescence resonance energy transfer (FRET) based “Turn-On” nanofluorescence sensor using a nitrogen-doped carbon dot-hexagonal cobalt oxyhydroxide nanosheet architecture and application to α -glucosidase inhibitor screening. *Biosens. Bioelectron.* **2016**, *79*, 728–735.
- (45) Boichenko, I.; Deiss, S.; Bär, K.; Hartmann, M. D.; Hernandez Alvarez, B. A FRET-Based Assay for the Identification and Characterization of Cereblon Ligands. *J. Med. Chem.* **2016**, *59*, 770–774.
- (46) Ma, F.; Liu, W.-j.; Tang, B.; Zhang, C.-y. A single quantum dot-based nanosensor for the signal-on detection of DNA methyltransferase. *Chem. Commun.* **2017**, *53*, 6868–6871.
- (47) Zhou, X.; Zhao, M.; Duan, X.; Guo, B.; Cheng, W.; Ding, S.; Ju, H. Collapse of DNA Tetrahedron Nanostructure for “Off-On” Fluorescence Detection of DNA Methyltransferase Activity. *ACS Appl. Mater. Interfaces* **2017**, *9*, 40087–40093.
- (48) Wang, Q.; Pan, M.; Wei, J.; Liu, X.; Wang, F. Evaluation of DNA Methyltransferase Activity and Inhibition via Isothermal Enzyme-Free Concatenated Hybridization Chain Reaction. *ACS Sensors* **2017**, *2*, 932–939.
- (49) Zhao, C.; Fan, J.; Peng, L.; Zhao, L.; Tong, C.; Wang, W.; Liu, B. An end-point method based on graphene oxide for RNase H analysis and inhibitors screening. *Biosens. Bioelectron.* **2017**, *90*, 103–109.
- (50) Tong, C.; Zhao, C.; Liu, B.; Li, B.; Ai, Z.; Fan, J.; Wang, W. Sensitive detection of RNase A activity and collaborative drug screening based on rGO and fluorescence probe. *Anal. Chem.* **2018**, *90*, 2655–2661.
- (51) Lee, J.; Samson, A. A. S.; Song, J. M. Inkjet printing-based β -secretase fluorescence resonance energy transfer (FRET) assay for screening of potential β -secretase inhibitors of Alzheimer’s disease. *Anal. Chim. Acta* **2018**, *1022*, 89–95.
- (52) Liu, Q.; Li, N.; Wang, M.; Wang, L.; Su, X. A label-free fluorescent biosensor for the detection of protein kinase activity based on gold nanoclusters/graphene oxide hybrid materials. *Anal. Chim. Acta* **2018**, *1013*, 71–78.
- (53) Lee, H. J.; Lee, Y. G.; Kang, J.; Yang, S. H.; Kim, J. H.; Ghisaidoobe, A. B. T.; Kang, H. J.; Lee, S.-R.; Lim, M. H.; Chung, S. J. Monitoring metal–amyloid- β complexation by a FRET-based probe:

- design, detection, and inhibitor screening. *Chem. Sci.* **2019**, *10*, 1000–1007.
- (54) Zhang, F.; Sun, Z.; Liao, L.; Zuo, Y.; Zhang, D.; Wang, J.; Chen, Y.; Xiao, S.; Jiang, H.; Lu, T.; Xu, P.; Yue, L.; Du, D.; Zhang, H.; Liu, C.; Luo, C. Discovery of novel CBP bromodomain inhibitors through TR-FRET-based high-throughput screening. *Acta Pharmacol. Sin.* **2020**, *41*, 286–292.
- (55) Senarisoy, M.; Barette, C.; Lacroix, F.; De Bonis, S.; Stelter, M.; Hans, F.; Kleman, J.-P.; Fauvarque, M.-O.; Timmins, J. Förster Resonance Energy Transfer Based Biosensor for Targeting the hNTH1–YB1 Interface as a Potential Anticancer Drug Target. *ACS Chem. Biol.* **2020**, *15*, 990–1003.
- (56) Stroik, D. R.; Yuen, S. L.; Janicek, K. A.; Schaaf, T. M.; Li, J.; Ceholski, D. K.; Hajjar, R. J.; Cornea, R. L.; Thomas, D. D. Targeting protein-protein interactions for therapeutic discovery via FRET-based high-throughput screening in living cells. *Sci. Rep.* **2018**, *8*, 12560.
- (57) Chen, T.; He, B.; Tao, J.; He, Y.; Deng, H.; Wang, X.; Zheng, Y. Application of Förster Resonance Energy Transfer (FRET) technique to elucidate intracellular and In Vivo biofate of nanomedicines. *Adv. Drug Delivery Rev.* **2019**, *143*, 177–205.
- (58) Kowada, T.; Maeda, H.; Kikuchi, K. BODIPY-based probes for the fluorescence imaging of biomolecules in living cells. *Chem. Soc. Rev.* **2015**, *44*, 4953–4972.
- (59) Sharma, K. K.; Przybilla, F.; Restle, T.; Boudier, C.; Godet, J.; Mély, Y. Reverse Transcriptase in Action: FRET-Based Assay for Monitoring Flipping and Polymerase Activity in Real Time. *Anal. Chem.* **2015**, *87*, 7690–7697.
- (60) Scholler, P.; Moreno-Delgado, D.; Lecat-Guillet, N.; Doumazane, E.; Monnier, C.; Charrier-Savournin, F.; Fabre, L.; Chouvet, C.; Soldevila, S.; Lamarque, L.; Donsimoni, G.; Roux, T.; Zwier, J. M.; Trinquet, E.; Rondard, P.; Pin, J.-P. HTS-compatible FRET-based conformational sensors clarify membrane receptor activation. *Nat. Chem. Biol.* **2017**, *13*, 372.
- (61) Luo, J.; Xie, Z.; Lam, J. W. Y.; Cheng, L.; Chen, H.; Qiu, C.; Kwok, H. S.; Zhan, X.; Liu, Y.; Zhu, D.; Tang, B. Z. Aggregation-induced emission of 1-methyl-1,2,3,4,5-pentaphenylsilole. *Chem. Commun.* **2001**, 1740–1741.
- (62) Mei, J.; Leung, N. L. C.; Kwok, R. T. K.; Lam, J. W. Y.; Tang, B. Z. Aggregation-Induced Emission: Together We Shine, United We Soar! *Chem. Rev.* **2015**, *115*, 11718–11940.
- (63) An, B.-K.; Kwon, S.-K.; Jung, S.-D.; Park, S. Y. Enhanced Emission and Its Switching in Fluorescent Organic Nanoparticles. *J. Am. Chem. Soc.* **2002**, *124*, 14410–14415.
- (64) Chen, J.; Law, C. C. W.; Lam, J. W. Y.; Dong, Y.; Lo, S. M. F.; Williams, I. D.; Zhu, D.; Tang, B. Z. Synthesis, Light Emission, Nanoaggregation, and Restricted Intramolecular Rotation of 1,1-Substituted 2,3,4,5-Tetraphenylsiloles. *Chem. Mater.* **2003**, *15*, 1535–1546.
- (65) Yuan, W. Z.; Lu, P.; Chen, S.; Lam, J. W. Y.; Wang, Z.; Liu, Y.; Kwok, H. S.; Ma, Y.; Tang, B. Z. Changing the Behavior of Chromophores from Aggregation-Caused Quenching to Aggregation-Induced Emission: Development of Highly Efficient Light Emitters in the Solid State. *Adv. Mater.* **2010**, *22*, 2159–2163.
- (66) Luo, J.; Song, K.; Gu, F. I.; Miao, Q. Switching of non-helical overcrowded tetrabenzooheptafulvalene derivatives. *Chem. Sci.* **2011**, *2*, 2029–2034.
- (67) Chen, L.; Jiang, Y.; Nie, H.; Lu, P.; Sung, H. H. Y.; Williams, I. D.; Kwok, H. S.; Huang, F.; Qin, A.; Zhao, Z.; Tang, B. Z. Creation of Bifunctional Materials: Improve Electron-Transporting Ability of Light Emitters Based on AIE-Active 2,3,4,5-Tetraphenylsiloles. *Adv. Funct. Mater.* **2014**, *24*, 3621–3630.
- (68) Shi, H.; Kwok, R. T. K.; Liu, J.; Xing, B.; Tang, B. Z.; Liu, B. Real-time monitoring of cell apoptosis and drug screening using fluorescent light-up probe with aggregation-induced emission characteristics. *J. Am. Chem. Soc.* **2012**, *134*, 17972–17981.
- (69) Yuan, Y.; Kwok, R. T. K.; Tang, B. Z.; Liu, B. Targeted theranostic platinum(IV) prodrug with a built-in aggregation-induced emission light-up apoptosis sensor for noninvasive early evaluation of its therapeutic responses in situ. *J. Am. Chem. Soc.* **2014**, *136*, 2546–2554.
- (70) Dhara, K.; Hori, Y.; Baba, R.; Kikuchi, K. A fluorescent probe for detection of histone deacetylase activity based on aggregation-induced emission. *Chem. Commun.* **2012**, *48*, 11534–11536.
- (71) Wang, H.; Huang, Y.; Zhao, X.; Gong, W.; Wang, Y.; Cheng, Y. A novel aggregation-induced emission based fluorescent probe for an angiotensin converting enzyme (ACE) assay and inhibitor screening. *Chem. Commun.* **2014**, *50*, 15075–15078.
- (72) Zhuang, Y.; Huang, F.; Xu, Q.; Zhang, M.; Lou, X.; Xia, F. Facile, Fast-Responsive, and Photostable Imaging of Telomerase Activity in Living Cells with a Fluorescence Turn-On Manner. *Anal. Chem.* **2016**, *88*, 3289–3294.
- (73) Wang, Y.; Chen, Y.; Wang, H.; Cheng, Y.; Zhao, X. Specific turn-on fluorescent probe with aggregation-induced emission characteristics for SIRT1 modulator screening and living-cell imaging. *Anal. Chem.* **2015**, *87*, 5046–5049.
- (74) Shen, W.; Yu, J.; Ge, J.; Zhang, R.; Cheng, F.; Li, X.; Fan, Y.; Yu, S.; Liu, B.; Zhu, Q. Light-Up Probes Based on Fluorogens with Aggregation-Induced Emission Characteristics for Monoamine Oxidase-A Activity Study in Solution and in Living Cells. *ACS Appl. Mater. Interfaces* **2016**, *8*, 927–935.
- (75) Wang, Y.; Wu, X.; Cheng, Y.; Zhao, X. A fluorescent switchable AIE probe for selective imaging of dipeptidyl peptidase-4 in vitro and in vivo and its application in screening DPP-4 inhibitors. *Chem. Commun.* **2016**, *52*, 3478–3481.
- (76) Lin, H.; Yang, H.; Huang, S.; Wang, F.; Wang, D.-M.; Liu, B.; Tang, Y.-D.; Zhang, C.-J. Caspase-1 specific light-up probe with aggregation-induced emission characteristics for inhibitor screening of coumarin-originated natural products. *ACS Appl. Mater. Interfaces* **2018**, *10*, 12173–12180.
- (77) Liu, G.; Wang, B.; Zhang, Y.; Xing, G.; Yang, X.; Wang, S. A tetravalent sialic acid-coated tetraphenylethene luminogen with aggregation-induced emission characteristics: design, synthesis and application for sialidase activity assay, high-throughput screening of sialidase inhibitors and diagnosis of bacterial vaginosis. *Chem. Commun.* **2018**, *54*, 10691–10694.
- (78) Atanasov, A. G.; Zotchev, S. B.; Dirsch, V. M.; et al. Natural products in drug discovery: advances and opportunities. *Nat. Rev. Drug Discovery* **2021**, *20*, 200–216.
- (79) Mayer-Wrangowski, S. C.; Rauh, D. Monitoring Ligand-Induced Conformational Changes for the Identification of Estrogen Receptor Agonists and Antagonists. *Angew. Chem., Int. Ed.* **2015**, *54*, 4379–4382.
- (80) Li, L.; Shi, W.; Wu, X.; Gong, Q.; Li, X.; Ma, H. Monitoring γ -glutamyl transpeptidase activity and evaluating its inhibitors by a water-soluble near-infrared fluorescent probe. *Biosens. Bioelectron.* **2016**, *81*, 395–400.
- (81) Feng, L.; Yang, Y.; Huo, X.; Tian, X.; Feng, Y.; Yuan, H.; Zhao, L.; Wang, C.; Chu, P.; Long, F.; Wang, W.; Ma, X. Highly Selective NIR Probe for Intestinal β -Glucuronidase and High-Throughput Screening Inhibitors to Therapy Intestinal Damage. *ACS Sensors* **2018**, *3*, 1727–1734.
- (82) Lei, Z.; Chen, H.; Zhang, H.; Wang, Y.; Meng, X.; Wang, Z. Evaluation of matrix metalloproteinase inhibition by peptide microarray-based fluorescence assay on polymer brush substrate and in vivo assessment. *ACS Appl. Mater. Interfaces* **2017**, *9*, 44241–44250.
- (83) Wang, H.; Li, Y.; Zhao, K.; Chen, S.; Wang, Q.; Lin, B.; Nie, Z.; Yao, S. G-quadruplex-based fluorometric biosensor for label-free and homogenous detection of protein acetylation-related enzymes activities. *Biosens. Bioelectron.* **2017**, *91*, 400–407.
- (84) Maity, S.; Sadlowski, C. M.; George Lin, J. M.; Chen, C. H.; Peng, L. H.; Lee, E. S.; Vegesna, G. K.; Lee, C.; Kim, S. H.; Mochly-Rosen, D.; Kumar, S.; Murthy, N. Thiophene bridged aldehydes (TBAs) image ALDH activity in cells via modulation of intramolecular charge transfer. *Chem. Sci.* **2017**, *8*, 7143–7151.
- (85) Hu, Y.; Miao, Z. Y.; Zhang, X. J.; Yang, X. T.; Tang, Y. Y.; Yu, S.; Shan, C. X.; Wen, H. M.; Zhu, D. Preparation of microkernel-based mesoporous (SiO₂-CdTe-SiO₂)@SiO₂ fluorescent nano-

particles for imaging screening and enrichment of heat shock protein 90 inhibitors from *Tripterygium Wilfordii*. *Anal. Chem.* **2018**, *90*, 5678–5686.

(86) Yeo, D. C.; Wiraja, C.; Miao, Q.; Ning, X.; Pu, K.; Xu, C. Anti-Scarring Drug Screening with Near-Infrared Molecular Probes Targeting Fibroblast Activation Protein- α . *ACS Applied Bio Materials* **2018**, *1*, 2054–2061.

(87) Peng, M.; Wang, Y.; Fu, Q.; Sun, F.; Na, N.; Ouyang, J. Melanosome-targeting near-infrared fluorescent probe with large Stokes shift for in situ quantification of tyrosinase activity and assessing drug effects on differently invasive melanoma cells. *Anal. Chem.* **2018**, *90*, 6206–6213.

(88) Liu, G.; Zhao, J.; Lu, S.; Wang, S.; Sun, J.; Yang, X. Polymethylidopa Nanoparticles-Based Fluorescent Sensor for Detection of Tyrosinase Activity. *ACS Sensors* **2018**, *3*, 1855–1862.

(89) Xu, X.; Kuang, Z.; Han, J.; Meng, Y.; Li, L.; Luan, H.; Xu, P.; Wang, J.; Luo, C.; Ding, H.; Li, Z.; Bian, J. Development and Characterization of a Fluorescent Probe for GLS1 and the Application for High-Throughput Screening of Allosteric Inhibitors. *J. Med. Chem.* **2019**, *62*, 9642–9657.

(90) Kawaguchi, M.; Han, X.; Hisada, T.; Nishikawa, S.; Kano, K.; Ieda, N.; Aoki, J.; Toyama, T.; Nakagawa, H. Development of an ENPP1 Fluorescence Probe for Inhibitor Screening, Cellular Imaging, and Prognostic Assessment of Malignant Breast Cancer. *J. Med. Chem.* **2019**, *62*, 9254–9269.

(91) Kawaguchi, M.; Ieda, N.; Nakagawa, H. Development of Peptide-Based Sirtuin Defatty-Acylase Inhibitors Identified by the Fluorescence Probe, SFP3, That Can Efficiently Measure Defatty-Acylase Activity of Sirtuin. *J. Med. Chem.* **2019**, *62*, 5434–5452.

(92) Zhang, D.; Meng, Y. R.; Zhang, C. Y. Peptide-templated gold nanoparticle nanosensor for simultaneous detection of multiple posttranslational modification enzymes. *Chem. Commun.* **2020**, *56*, 213–216.

(93) Li, L.; Feng, L.; Zhang, M.; He, X.; Luan, S.; Wang, C.; James, T. D.; Zhang, H.; Huang, H.; Ma, X. Visualization of penicillin G acylase in bacteria and high-throughput screening of natural inhibitors using a ratiometric fluorescent probe. *Chem. Commun.* **2020**, *56*, 4640–4643.

(94) Zhang, L.; Wei, M.; Gao, C.; Wei, W.; Zhang, Y.; Liu, S. Label-free electrochemical detection of methyltransferase activity and inhibitor screening based on endonuclease HpaII and the deposition of polyaniline. *Biosens. Bioelectron.* **2015**, *73*, 188–194.

(95) Peng, X.; Zhu, J.; Wen, W.; Bao, T.; Zhang, X.; He, H.; Wang, S. Silver nanoclusters-assisted triple-amplified biosensor for ultrasensitive methyltransferase activity detection based on AuNPs/ERGO hybrids and hybridization chain reaction. *Biosens. Bioelectron.* **2018**, *118*, 174–180.

(96) Gu, C.; Gai, P.; Kong, X.; Hou, T.; Li, F. Self-powered biosensing platform based on “Signal-On” enzymatic biofuel cell for DNA methyltransferase activity analysis and inhibitor screening. *Anal. Chem.* **2020**, *92*, 5426–5430.

(97) Yin, H.; Wang, M.; Li, B.; Yang, Z.; Zhou, Y.; Ai, S. A sensitive electrochemical biosensor for detection of protein kinase A activity and inhibitors based on Phos-tag and enzymatic signal amplification. *Biosens. Bioelectron.* **2015**, *63*, 26–32.

(98) Shen, C.; Li, X.; Rasooly, A.; Guo, L.; Zhang, K.; Yang, M. A single electrochemical biosensor for detecting the activity and inhibition of both protein kinase and alkaline phosphatase based on phosphate ions induced deposition of redox precipitates. *Biosens. Bioelectron.* **2016**, *85*, 220–225.

(99) Zhao, J.; Yang, L.; Dai, Y.; Tang, Y.; Gong, X.; Du, D.; Cao, Y. Peptide-templated multifunctional nanoprobe for feasible electrochemical assay of intracellular kinase. *Biosens. Bioelectron.* **2018**, *119*, 42–47.

(100) Zhang, J.; Liu, Y.; Wang, X.; Chen, Y.; Li, G. Electrochemical assay of α -glucosidase activity and the inhibitor screening in cell medium. *Biosens. Bioelectron.* **2015**, *74*, 666–672.

(101) Xu, Y.; Liu, L.; Wang, Z.; Dai, Z. Stable and reusable electrochemical biosensor for poly(ADP-ribose) polymerase and its

inhibitor based on enzyme-initiated auto-PARylation. *ACS Appl. Mater. Interfaces* **2016**, *8*, 18669–18674.

(102) Hu, Q.; Bao, Y.; Gan, S.; Zhang, Y.; Han, D.; Niu, L. Amplified Electrochemical Biosensing of Thrombin Activity by RAFT Polymerization. *Anal. Chem.* **2020**, *92*, 3470–3476.

(103) Hu, D.; Hu, Y.; Zhan, T.; Zheng, Y.; Ran, P.; Liu, X.; Guo, Z.; Wei, W.; Wang, S. Coenzyme A-aptamer-facilitated label-free electrochemical stripping strategy for sensitive detection of histone acetyltransferase activity. *Biosens. Bioelectron.* **2020**, *150*, 111934.

(104) McCreery, R. L. Advanced Carbon Electrode Materials for Molecular Electrochemistry. *Chem. Rev.* **2008**, *108*, 2646–2687.

(105) Zhang, W.; Zhu, S.; Luque, R.; Han, S.; Hu, L.; Xu, G. Recent development of carbon electrode materials and their bioanalytical and environmental applications. *Chem. Soc. Rev.* **2016**, *45*, 715–752.

(106) Aymard, C. M. G.; Halma, M.; Comte, A.; Mousty, C.; Prévot, V.; Hecquet, L.; Charmantray, F.; Blum, L. J.; Doumèche, B. Innovative electrochemical screening allows transketolase inhibitors to be identified. *Anal. Chem.* **2018**, *90*, 9241–9248.

(107) Zhao, W.-W.; Xu, J.-J.; Chen, H.-Y. Photoelectrochemical enzymatic biosensors. *Biosens. Bioelectron.* **2017**, *92*, 294–304.

(108) Yang, Z.; Wang, F.; Wang, M.; Yin, H.; Ai, S. A novel signal-on strategy for M.SssI methyltransferase activity analysis and inhibitor screening based on photoelectrochemical immunosensor. *Biosens. Bioelectron.* **2015**, *66*, 109–114.

(109) Shen, Q.; Han, L.; Fan, G.; Abdel-Halim, E. S.; Jiang, L.; Zhu, J. Highly sensitive photoelectrochemical assay for DNA methyltransferase activity and inhibitor screening by exciton energy transfer coupled with enzyme cleavage biosensing strategy. *Biosens. Bioelectron.* **2015**, *64*, 449–455.

(110) Yin, H.; Sun, B.; Dong, L.; Li, B.; Zhou, Y.; Ai, S. A signal “on” photoelectrochemical biosensor for assay of protein kinase activity and its inhibitor based on graphite-like carbon nitride, Phos-tag and alkaline phosphatase. *Biosens. Bioelectron.* **2015**, *64*, 462–468.

(111) Wang, J.; Song, M.; Hu, C.; Wu, K. Portable, self-powered, and light-addressable photoelectrochemical sensing platforms using pH meter readouts for high-throughput screening of thrombin inhibitor drugs. *Anal. Chem.* **2018**, *90*, 9366–9373.

(112) Li, P.; Cao, Y.; Mao, C.; Jin, B.; Zhu, J. TiO₂/g-C₃N₄/CdS nanocomposite-based photoelectrochemical biosensor for ultrasensitive evaluation of T4 polynucleotide kinase activity. *Anal. Chem.* **2019**, *91*, 1563–1570.

(113) Vaquer, G.; Dannertstedt, F. R.; Mavris, M.; Bignami, F.; Llinares-Garcia, J.; Westermarck, K.; Sepodes, B. Animal models for metabolic, neuromuscular and ophthalmological rare diseases. *Nat. Rev. Drug Discovery* **2013**, *12*, 287–305.

(114) Weaver, R. J.; Blomme, E. A.; Chadwick, A. E.; Copple, I. M.; Gerets, H. H. J.; Goldring, C. E.; Guillouzo, A.; Hewitt, P. G.; Ingelman-Sundberg, M.; Jensen, K. G.; Juhila, S.; Klingmüller, U.; Labbe, G.; Liguori, M. J.; Lovatt, C. A.; Morgan, P.; Naisbitt, D. J.; Pieters, R. H. H.; Snoeys, J.; van de Water, B.; et al. Managing the challenge of drug-induced liver injury: a roadmap for the development and deployment of preclinical predictive models. *Nat. Rev. Drug Discovery* **2020**, *19*, 131–148.

(115) Nobis, M.; McGhee, E. J.; Morton, J. P.; Schwarz, J. P.; Karim, S. A.; Quinn, J.; Edward, M.; Campbell, A. D.; McGarry, L. C.; Evans, T. R.; Brunton, V. G.; Frame, M. C.; Carragher, N. O.; Wang, Y.; Sansom, O. J.; Timpson, P.; Anderson, K. I. Intravital FLIM-FRET imaging reveals dasatinib-induced spatial control of src in pancreatic cancer. *Cancer Res.* **2013**, *73*, 4674–4686.

(116) Gómez-Soler, M.; Fernández-Dueñas, V.; Portillo-Salido, E.; Pérez, P.; Zamanillo, D.; Vela, J. M.; Burgueño, J.; Ciruela, F. Predicting the antinociceptive efficacy of $\sigma(1)$ receptor ligands by a novel receptor fluorescence resonance energy transfer (FRET) based biosensor. *J. Med. Chem.* **2014**, *57*, 238–242.

(117) Kondo, T.; Fujioka, M.; Tsuda, M.; Murai, K.; Yamaguchi, K.; Miyagishima, T.; Shindo, M.; Nagashima, T.; Wakasa, K.; Fujimoto, N.; Yamamoto, S.; Yonezumi, M.; Saito, S.; Sato, S.; Ogawa, K.; Chou, T.; Watanabe, R.; Kato, Y.; Takahashi, S.; Okano, Y.; et al. Pretreatment evaluation of fluorescence resonance energy transfer

based drug sensitivity test for patients with chronic myelogenous leukemia treated with dasatinib. *Cancer Sci.* **2018**, *109*, 2256–2265.

(118) Horiguchi, M.; Fujioka, M.; Kondo, T.; Fujioka, Y.; Li, X.; Horiuchi, K.; Satoh, A. O.; Nepal, P.; Nishide, S.; Nanbo, A.; Teshima, T.; Ohba, Y. Improved FRET Biosensor for the Measurement of BCR-ABL Activity in Chronic Myeloid Leukemia Cells. *Cell Struct. Funct.* **2017**, *42*, 15–26.

(119) Kondo, T.; Fujioka, M.; Fujisawa, S.; Sato, K.; Tsuda, M.; Miyagishima, T.; Mori, A.; Iwasaki, H.; Kakinoki, Y.; Yamamoto, S.; Haseyama, Y.; Ando, S.; Shindo, M.; Ota, S.; Kurosawa, M.; Ohba, Y.; Teshima, T. Clinical efficacy and safety of first-line nilotinib therapy and evaluation of the clinical utility of the FRET-based drug sensitivity test. *Int. J. Hematol.* **2019**, *110*, 482–489.

(120) Contreras-Baeza, Y.; Ceballo, S.; Arce-Molina, R.; Sandoval, P. Y.; Alegria, K.; Barros, L. F.; San Martín, A. MitoToxy assay: A novel cell-based method for the assessment of metabolic toxicity in a multiwell plate format using a lactate FRET nanosensor, Laconic. *PLoS One* **2019**, *14*, e0224527.

(121) Gaborit, N.; Larbouret, C.; Vallaghe, J.; Peyrusson, F.; Bascoul-Mollevis, C.; Crapez, E.; Azria, D.; Chardès, T.; Poul, M. A.; Mathis, G.; Bazin, H.; Pèlerin, A. Time-resolved fluorescence resonance energy transfer (TR-FRET) to analyze the disruption of EGFR/HER2 dimers: a new method to evaluate the efficiency of targeted therapy using monoclonal antibodies. *J. Biol. Chem.* **2011**, *286*, 11337–11345.

(122) Chernov, K. G.; Redchuk, T. A.; Omelina, E. S.; Verkhusha, V. V. Near-Infrared Fluorescent Proteins, Biosensors, and Optogenetic Tools Engineered from Phytochromes. *Chem. Rev.* **2017**, *117*, 6423–6446.

(123) Duro-Castano, A.; Lim, N. H.; Tranchant, I.; Amoura, M.; Beau, F.; Wieland, H.; Kingler, O.; Herrmann, M.; Nazaré, M.; Plettenburg, O.; Dive, V.; Vicent, M. J.; Nagase, H. In vivo imaging of MMP-13 activity using a specific polymer-FRET peptide conjugate detects early osteoarthritis and inhibitor efficacy. *Adv. Funct. Mater.* **2018**, *28*, 1802738.

(124) Shuhendler, A. J.; Pu, K.; Cui, L.; Uetrecht, J. P.; Rao, J. Real-time imaging of oxidative and nitrosative stress in the liver of live animals for drug-toxicity testing. *Nat. Biotechnol.* **2014**, *32*, 373–380.

(125) Peng, J.; Samanta, A.; Zeng, X.; Han, S.; Wang, L.; Su, D.; Loong, D. T. B.; Kang, N.-Y.; Park, S.-J.; All, A. H.; Jiang, W.; Yuan, L.; Liu, X.; Chang, Y.-T. Real-time in vivo hepatotoxicity monitoring through chromophore-conjugated photon-upconverting nanoprobe. *Angew. Chem., Int. Ed.* **2017**, *56*, 4165–4169.

(126) Cheng, D.; Xu, W.; Yuan, L.; Zhang, X. Investigation of drug-induced hepatotoxicity and its remediation pathway with reaction-based fluorescent probes. *Anal. Chem.* **2017**, *89*, 7693–7700.

(127) Li, D.; Wang, S.; Lei, Z.; Sun, C.; El-Toni, A. M.; Alhoshan, M. S.; Fan, Y.; Zhang, F. Peroxynitrite activatable NIR-II fluorescent molecular probe for drug-Induced hepatotoxicity monitoring. *Anal. Chem.* **2019**, *91*, 4771–4779.

(128) Cheng, P.; Miao, Q.; Li, J.; Huang, J.; Xie, C.; Pu, K. Unimolecular chemo-fluoro-luminescent reporter for crosstalk-free duplex imaging of hepatotoxicity. *J. Am. Chem. Soc.* **2019**, *141*, 10581–10584.

(129) Cheng, D.; Peng, J.; Lv, Y.; Su, D.; Liu, D.; Chen, M.; Yuan, L.; Zhang, X. De novo design of chemical stability near-infrared molecular probes for high-fidelity hepatotoxicity evaluation in vivo. *J. Am. Chem. Soc.* **2019**, *141*, 6352–6361.

(130) Huang, J.; Li, J.; Lyu, Y.; Miao, Q.; Pu, K. Molecular optical imaging probes for early diagnosis of drug-induced acute kidney injury. *Nat. Mater.* **2019**, *18*, 1133–1143.

(131) Cheng, P.; Chen, W.; Li, S.; He, S.; Miao, Q.; Pu, K. Fluoro-Photoacoustic Polymeric Renal Reporter for Real-Time Dual Imaging of Acute Kidney Injury. *Adv. Mater.* **2020**, *32*, 1908530.

(132) Huang, J.; Xie, C.; Zhang, X.; Jiang, Y.; Li, J.; Fan, Q.; Pu, K. Renal-clearable Molecular Semiconductor for Second Near-Infrared Fluorescence Imaging of Kidney Dysfunction. *Angew. Chem., Int. Ed.* **2019**, *58*, 15120–15127.

(133) Wang, S.; Fan, Y.; Li, D.; Sun, C.; Lei, Z.; Lu, L.; Wang, T.; Zhang, F. Anti-quenching NIR-II molecular fluorophores for in vivo high-contrast imaging and pH sensing. *Nat. Commun.* **2019**, *10*, 1058.

(134) Kenry; Duan, Y.; Liu, B. Recent Advances of Optical Imaging in the Second Near-Infrared Window. *Adv. Mater.* **2018**, *30*, 1802394.

(135) Zhong, Y.; Ma, Z.; Wang, F.; Wang, X.; Yang, Y.; Liu, Y.; Zhao, X.; Li, J.; Du, H.; Zhang, M.; Cui, Q.; Zhu, S.; Sun, Q.; Wan, H.; Tian, Y.; Liu, Q.; Wang, W.; Garcia, K. C.; Dai, H. In vivo molecular imaging for immunotherapy using ultra-bright near-infrared-IIb rare-earth nanoparticles. *Nat. Biotechnol.* **2019**, *37*, 1322–1331.

(136) Miao, Q.; Pu, K. Organic Semiconducting Agents for Deep-Tissue Molecular Imaging: Second Near-Infrared Fluorescence, Self-Luminescence, and Photoacoustics. *Adv. Mater.* **2018**, *30*, 1801778.

(137) Wang, T.-T.; Wei, Q.-C.; Zhang, Z.-T.; Lin, M.-T.; Chen, J.-J.; Zhou, Y.; Guo, N.-N.; Zhong, X.-C.; Xu, W.-H.; Liu, Z.-X.; Han, M.; Gao, J.-Q. AIE/FRET-based versatile PEG-Pep-TPE/DOX nanoparticles for cancer therapy and real-time drug release monitoring. *Biomater. Sci.* **2020**, *8*, 118–124.

(138) Dong, Z.; Bi, Y.; Cui, H.; Wang, Y.; Wang, C.; Li, Y.; Jin, H.; Wang, C. AIE Supramolecular Assembly with FRET Effect for Visualizing Drug Delivery. *ACS Appl. Mater. Interfaces* **2019**, *11*, 23840–23847.

(139) Shih, H.-P.; Zhang, X.; Aronov, A. M. Drug discovery effectiveness from the standpoint of therapeutic mechanisms and indications. *Nat. Rev. Drug Discovery* **2018**, *17*, 19–33.

(140) Han, Y.; Duan, X.; Yang, L.; Nilsson-Payant, B. E.; Wang, P.; Duan, F.; Tang, X.; Yaron, T. M.; Zhang, T.; Uhl, S.; Bram, Y.; Richardson, C.; Zhu, J.; Zhao, Z.; Redmond, D.; Houghton, S.; Nguyen, D.-H. T.; Xu, D.; Wang, X.; Jessurun, J.; et al. Identification of SARS-CoV-2 inhibitors using lung and colonic organoids. *Nature* **2021**, *589*, 270–275.

(141) Vlachogiannis, G.; Hedayat, S.; Vatsiou, A.; Jamin, Y.; Fernández-Mateos, J.; Khan, K.; Lampis, A.; Eason, K.; Huntingford, I.; Burke, R.; Rata, M.; Koh, D.-M.; Tunariu, N.; Collins, D.; Hulkki-Wilson, S.; Ragulan, C.; Spiteri, I.; Moorcraft, S. Y.; Chau, I.; Rao, S.; et al. Patient-derived organoids model treatment response of metastatic gastrointestinal cancers. *Science* **2018**, *359*, 920.

(142) Esch, E. W.; Bahinski, A.; Huh, D. Organs-on-chips at the frontiers of drug discovery. *Nat. Rev. Drug Discovery* **2015**, *14*, 248–260.